Inorganic Chemistry
Article

Inorg. Chem. **2011**, *50*, 1275–1287 **1275**
DOI: 10.1021/ic101799c

Synthesis and Physicochemical Characterization of Carbon Backbone Modified $[Gd(TTDA)(H_2O)]^{2-}$ Derivatives

Ya-Hui Chang,[†] Chiao-Yun Chen,[‡,§] Gyan Singh,[∥] Hsing-Yin Chen,[†] Gin-Chung Liu,[‡,§] Yih-Gang Goan,[#,▽] Silvio Aime,[○] and Yun-Ming Wang*[,∥,⊥]

[†]*Department of Medicinal and Applied Chemistry,* [‡]*Department of Medical Imaging, Kaohsiung Medical University Hospital,* [§]*Department of Radiology, Kaohsiung Medical University, 100 Shih-Chuan first Road, Kaohsiung 807, Taiwan,* [∥]*Department of Biological Science and Technology, and* [⊥]*Institute of Molecular Medicine and Bioengineering, National Chiao Tung University, 75 Bo-Ai Street, Hsinchu 300, Taiwan,* [#]*Department of Surgery, Kaohsiung Veterans General Hospital, Kaohsiung, Taiwan,* [▽]*Department of Nursing, Yuh-Ing Junior College of Health Care & Management, Kaohsiung, Taiwan, and* [○]*Department of Chemistry IFM and Molecular Imaging Center, University of Torino, Torino, Italy*

Received September 2, 2010

The present study was designed to exploit optimum lipophilicity and high water-exchange rate (k_{ex}) on low molecular weight Gd(III) complexs to generate high bound relaxivity (r_1^b), upon binding to the lipophilic site of human serum albumin (HSA). Two new carbon backbone modified TTDA (3,6,10-tri(carboxymethyl)-3,6,10-triazadodecanedioic acid) derivatives, CB-TTDA and Bz-CB-TTDA, were synthesized. The complexes $[Gd(CB\text{-}TTDA)(H_2O)]^{2-}$ and $[Gd(Bz\text{-}CB\text{-}TTDA)(H_2O)]^{2-}$ both display high stability constant ($\log K_{GdL} = 20.28$ and 20.09, respectively). Furthermore, CB-TTDA ($\log K_{(Gd/Zn)} = 4.22$) and Bz-CB-TTDA ($\log K_{(Gd/Zn)} = 4.12$) exhibit superior selectivity of Gd(III) against Zn(II) than those of TTDA ($\log K_{(Gd/Zn)} = 2.93$), EPTPA-bz-NO_2 ($\log K_{(Gd/Zn)} = 3.19$), and DTPA ($\log K_{(Gd/Zn)} = 3.76$). However, the stability constant values of $[Gd(CB\text{-}TTDA)(H_2O)]^{2-}$ and $[Gd(Bz\text{-}CB\text{-}TTDA)(H_2O)]^{2-}$ are lower than that of MS-325. The parameters that affect proton relaxivity have been determined in a combined variable temperature ^{17}O NMR and NMRD study. The water exchange rates are comparable for the two complexes, $232 \times 10^6\ s^{-1}$ for $[Gd(CB\text{-}TTDA)(H_2O)]^{2-}$ and $271 \times 10^6\ s^{-1}$ for $[Gd(Bz\text{-}CB\text{-}TTDA)(H_2O)]^{2-}$. They are higher than those of $[Gd(TTDA)(H_2O)]^{2-}$ ($146 \times 10^6\ s^{-1}$), $[Gd(DTPA)(H_2O)]^{2-}$ ($4.1 \times 10^6\ s^{-1}$), and MS-325 ($6.1 \times 10^6\ s^{-1}$). Elevated stability and water exchange rate indicate that the presence of cyclobutyl on the carbon backbone imparts rigidity and steric constraint to $[Gd(CB\text{-}TTDA)(H_2O)]^{2-}$and $[Gd(Bz\text{-}CB\text{-}TTDA)(H_2O)]^{2-}$. In addition, the major objective for selecting the cyclobutyl is to tune the lipophilicity of $[Gd(Bz\text{-}CB\text{-}TTDA)(H_2O)]^{2-}$. The binding affinity of $[Gd(Bz\text{-}CB\text{-}TTDA)(H_2O)]^{2-}$ to HSA was evaluated by ultrafiltration study across a membrane with a 30 kDa MW cutoff, and the first three stepwise binding constants were determined by fitting the data to a stoichiometric model. The binding association constants (K_A) for $[Gd(CB\text{-}TTDA)(H_2O)]^{2-}$ and $[Gd(Bz\text{-}CB\text{-}TTDA)(H_2O)]^{2-}$ are 1.1×10^2 and 1.5×10^3, respectively. Although the K_A value for $[Gd(Bz\text{-}CB\text{-}TTDA)(H_2O)]^{2-}$ is lower than that of MS-325 ($K_A = 3.0 \times 10^4$), the r_1^b value, $r_1^b = 66.7\ mM^{-1}\ s^{-1}$ for $[Gd(Bz\text{-}CB\text{-}TTDA)(H_2O)]^{2-}$, is significantly higher than that of MS-325 ($r_1^b = 47.0\ mM^{-1}\ s^{-1}$). As measured by the Zn(II) transmetalation process, the kinetic stabilities of $[Gd(CB\text{-}TTDA)(H_2O)]^{2-}$, $[Gd(Bz\text{-}CB\text{-}TTDA)(H_2O)]^{2-}$, and $[Gd(DTPA)(H_2O)]^{2-}$ are similar and are significantly higher than that of $[Gd(DTPA\text{-}BMA)(H_2O)]^{2-}$. High thermodynamic and kinetic stability and optimized lipophilicity of $[Gd(CB\text{-}TTDA)(H_2O)]^{2-}$ make it a favorable blood pool contrast agent for MRI.

Introduction

Magnetic resonance imaging (MRI) has proven invaluable in the clinical imaging of several anatomical and physiological abnormalities. The technique exploits in vivo water present in tissue at ~90 M to increase contrast between normal and abnormal tissue.[1] The major disadvantage of MRI is its inherent low sensitivity. To enhance the quality of image, contrast agents (CAs) have often been used prior to MR imaging, which serve as catalysts in shortening the

*To whom correspondence should be addressed. Mailing address: Department of Biological Science and Technology, Institute of Molecular Medicine and Bioengineering, National Chiao Tung University, 75 Bo-Ai Street, Hsinchu 300, Taiwan. Telephone: 886-3-5721212 ext 56972. Fax: 886-3-5729288. E-mail:ymwang@mail.nctu.edu.tw.

(1) Caravan, P. *Chem. Soc. Rev.* **2006**, *35*, 512–523.
(2) (a) Polášek, M.; Šedinová, M.; Kotek, J.; Vander Elst, L.; Muller, R. N.; Hermann, P.; Lukeš, I. *Inorg. Chem.* **2009**, *48*, 455–465. (b) Frangioni, J. V. *Nat. Biotechnol.* **2006**, *24*, 909–913. (c) Louie, A. Y.; Huber, M. M.; Ahrens, E. T.; Rothbacher, U.; Moats, R.; Jacobs, R. E.; Fraser, S. E.; Meade, T. J. *Nat. Biotechnol.* **2000**, *18*, 321–325.

Published on Web 01/19/2011

longitudinal and transverse relaxation time (i.e., T_1 and T_2) of water protons.[2] Primary clinical CAs, such as [Gd(DTPA)(H_2O)]$^{2-}$ (Magnevist), [Gd(DTPA-BMA)(H_2O)] (Omniscan), and [Gd(DOTA)(H_2O)]$^-$ (Dotarem), display relaxivities of around 4−5 mM^{-1} s^{-1} in the range of magnetic fields (0.5−1.5 T) used in clinical MRI at 37 °C.[3] However, the Solomon−Bloembergen−Morgan (SBM) theory predicts an over 20-fold relaxivity enhancement for the Gd(III) complex with single hydration state ($q = 1$) at regular imaging fields used for clinical imaging, upon the simultaneous optimization of key parameters, such as the electronic relaxation rate ($1/T_{1,2e}$), the water exchange rate (k_{ex}), and the molecular rotational correlation time (τ_R).[4,5] However, in practice, the electronic relaxation rate ($1/T_{1,2e}$) of the paramagnetic center is still hard to alter.[3]

In the past few years many endeavors have been made to develop hypersensitive CAs. In this front, CAs endowed with much higher relaxivity,[6] targeting specific organ and tissue,[7] and behaving as smart CAs[8] have been extensively explored. Recently, special attention has been devoted to the optimization of water exchange rate on Gd(III) complexes.[9−11] The inner-sphere water exchange rate has been shown to reach its optimal value when steric compression is created around the water binding site in the Gd(III) complex.[12] Steric crowding facilitates in squeezing out the bound water molecules in the rate determining step and consequently accelerates the water exchange. This phenomenon has been observed in both acyclic[13] and macrocyclic[14] Gd(III) complexes. However, for low molecular weight Gd(III) complexes, high water exchange rate has only limited advantages since relaxivity is mainly restricted by fast molecular motion.[15] T_1 relaxation is optimum when the frequency of molecular motion is close to the Larmor frequency. However, the small gadolinium complexes are characterized by rotational correlation times ranging between 50 and 100 ps, which corresponds to rotational frequencies of 10−20 GHz in contrast to the optimal imaging field strength for clinical imaging ranging from 0.5 to 1.5 T which corresponds to Lamor frequencies of 20−65 MHz.[16] Fortunately, it is well established from previous studies that the metal complex fluctuates at frequency somewhat closer to the proton Larmor frequency on slowing down rotational diffusion and, consequently, relaxivity gain can be achieved.[17] A systematic review identifies a number of strategies employed to design high molecular weight CAs. Small molecular weight Gd(III) complexes can be covalently or noncovalently bound to macromolecules, for instance, linear polymers,[18] dendrimers,[19] viral capsids,[20] proteins,[21] polysaccharides,[22] DNA quadruplex scaffolds,[23] self- assembled peptide amphiphile nanofibers,[24] and liposomes.[25] However, some of these approaches suffer from internal flexibility or nonrigid attachment of ligand to macromolecule.[26] Noncovalent interaction of small Gd(III) complexes to in vivo proteins has drawn much attention due to diverse physiological congenial reasons. This approach is often called receptor-induced magnetization enhancement (RIME).[27] The commercial contrast agent MS-325 (Vasovist) is an example of a rationally designed RIME CA for angiographic application. It possesses a lipophilic diphenylcyclohexyl residue which facilitates noncovalent interaction with human serum albumin (HSA).[28,29] The binding augments the blood plasma circulation time and also slows down its tumbling rate, leading to greater contrast enhancements of blood vessel MR image.[30] It is apparent from previous studies that

(3) Costa, J.; Tóth, É.; Helm, L.; Merbach, A. E. *Inorg. Chem.* **2005**, *44*, 4747–4755.
(4) Solomon, I. *Phys. Rev.* **1955**, *99*, 559–565.
(5) Bloembergen, N.; Morgan, L. O. *J. Chem. Phys.* **1961**, *34*, 842–850.
(6) (a) Fatin-Rouge, N.; Tóth, E.; Meuli, R.; Bünzli, J. C. G. *J. Alloys Compd.* **2004**, *374*, 298–302. (b) Vander Elst, L.; Port, M.; Raynal, I.; Simonot, C.; Muller, R. N. *Eur. J. Inorg. Chem.* **2003**, 2495–2501. (c) Aime, S.; Cabella, C.; Colombatto, S.; Crich, S. G.; Gianolio, E.; Maggioni, F. *J. Magn. Reson. Imaging* **2002**, *16*, 394–406.
(7) (a) Weinmann, H. J.; Ebert, W.; Misselwitz, B.; Schmitt-Willich, H. *Eur. J. Radiol.* **2003**, *46*, 33–44. (b) Kubíček, V.; Rudovský, J.; Kotek, J.; Hermann, P.; Vander Elst, L.; Muller, R. N.; Kolar, Z. I.; Wolterbeek, H. T.; Peters, J. A.; Lukeš, I. *J. Am. Chem. Soc.* **2005**, *127*, 16477–16485.
(8) (a) Chang, Y. T.; Cheng, C. M.; Su, Y. Z.; Lee, W. T.; Hsu, J. S.; Liu, G. C.; Cheng, T. L.; Wang, Y. M. *Bioconjugate Chem.* **2007**, *18*, 1716–1727. (b) Duimstra, J. A.; Femia, F. J.; Meade, T. J. *J. Am. Chem. Soc.* **2005**, 12847–12855.
(9) Wang, Y. M.; Lee, C. H.; Liu, G. C.; Sheu, R. S. *Dalton Trans.* **1998**, *24*, 4113–4118.
(10) Mato-Iglesias, M.; Platas-Iglesias, C.; Djanashvili, K.; Peters, J. A.; Tóth, É.; Balogh, E.; Muller, R. N.; Vander Elst, L.; de Blas, A.; Rodríguez-Blas, T. *Chem. Commun.* **2005**, 4729–4731.
(11) Balogh, E.; Mato-Iglesias, M.; Platas-Iglesias, C.; Tóth, E.; Djanashvili, K.; Peters, J. A.; de Blas, A.; Rodríguez-Blas, T. *Inorg. Chem.* **2006**, *45*, 8719–8728.
(12) Powell, D. H.; Ni Dhubhghaill, O. M.; Pubanz, D.; Helm, L.; Lebedev, Y. S.; Schlaepfer, W.; Merbach, A. E. *J. Am. Chem. Soc.* **1996**, *118*, 9333–9346.
(13) Aime, S.; Barge, A.; Borel, A.; Botta, M.; Chemerisov, S.; Merbach, A. E.; Müller, U.; Pubanz, D. *Inorg. Chem.* **1997**, *36*, 5104–5112.
(14) Ruloff, R.; Tóth, É.; Scopelliti, R.; Tripier, R.; Handel, H.; Merbach, A. E. *Chem. Commun.* **2002**, 2630–2631.
(15) Burai, L.; Tóth, E.; Sour, A.; Merbach, A. E. *Inorg. Chem.* **2005**, *44*, 3561–3568.
(16) Caravan, P.; Cloutier, N. J.; Greenfield, M. T.; McDermid, S. A.; Dunham, S. U.; Bulte, J. W.; Amedio, J. C., Jr.; Looby, R. J.; Supkowski, R. M.; Horrocks, W. D., Jr.; McMurry, T. J.; Lauffer, R. B. *J. Am. Chem. Soc.* **2002**, *124*, 3152–3162.
(17) (a) Lauffer, R. B.; Brady, T. *J. Magn. Reson. Imaging* **1985**, *3*, 11–16. (b) Lauffer, R. B.; Brady, T. J.; Brown, R. D., III; Baglin, C.; Koenig, S. H. *Magn. Reson. Med.* **1986**, *3*, 541–548.
(18) (a) Lucas, R. L.; Benjamin, M.; Reineke, T. M. *Bioconjugate Chem.* **2008**, *19*, 24–27. (b) Zhang, G.; Zhang, R.; Wen, X.; Li, L.; Li, C. *Biomacromolecules* **2008**, *9*, 36–42. (c) Fu, Y.; Raatschen, H. J.; Nitecki, D. E.; Wendland, M. F.; Novikov, V.; Fournier, L. S.; Cyran, C.; Rogut, V.; Shames, D. M.; Brasch, R. C. *Biomacromolecules* **2007**, *8*, 1519–1529.
(19) Xu, H.; Regino, C. A.; Koyama, Y.; Hama, Y.; Gunn, A. J.; Bernardo, M.; Kobayashi, H.; Choyke, P. L.; Brechbiel, M. W. *Bioconjugate Chem.* **2007**, *18*, 1474–1482.
(20) Anderson, E. A.; Isaacman, S.; Peabody, D. S.; Wang, E. Y.; Canary, J. W.; Kirshenbaum, K. *Nano Lett.* **2006**, *6*, 1160–1164.
(21) (a) Yang, J. J.; Yang, J.; Wei, L.; Zurkiya, O.; Yang, W.; Li, S.; Zou, J.; Zhou, Y.; Maniccia, A. L.; Mao, H.; Zhao, F.; Malchow, R.; Zhao, S.; Johnson, J.; Hu, X.; Krogstad, E.; Liu, Z. R. *J. Am. Chem. Soc.* **2008**, *130*, 9260–9267. (b) Karfeld, L. S.; Bull, S. R.; Davis, N. E.; Meade, T. J.; Barron, A. E. *Bioconjugate Chem.* **2007**, *18*, 1697–1700.
(22) Sirlin, C. B.; Vera, D. R.; Corbeil, J. A.; Caballero, M. B.; Buxton, R. B.; Mattrey, R. F. *Acad. Radiol.* **2004**, *11*, 1361–1369.
(23) Cai, J.; Shapiro, E. M.; Hamilton, A. D. *Bioconjugate Chem.* **2009**, *20*, 205–208.
(24) Bull, S. R.; Guler, M. O.; Bras, R. E.; Meade, T. J.; Stupp, S. I. *Nano Lett.* **2005**, *5*, 1–4.
(25) (a) Laurent, S.; Vander Elst, L.; Thirifays, C.; Muller, R. N. *Langmuir* **2008**, *24*, 4347–4351. (b) Laurent, Vander Elst, L.; Thirifays, C.; Muller, R. N. *Eur. Biophys. J.* **2008**, *37*, 1007–1014.
(26) (a) Hermann, P.; Kotek, J.; Kubíček, V.; Lukeš, I. *Dalton Trans.* **2008**, 3027–3047. (b) Jászberényi, Z.; Moriggi, L.; Schmidt, P.; Weidensteiner, C.; Kneuer, R.; Merbach, A. E.; Helm, L.; Tóth, É. *J. Biol. Inorg. Chem.* **2007**, *12*, 406–420. (c) Rudovský, J.; Botta, M.; Hermann, P.; Hardcastle, K. I.; Lukeš, I.; Aime, S. *Bioconjugate Chem.* **2006**, *17*, 975–987.
(27) (a) Jenkins, B. G.; Armstrong, E.; Lauffer, R. B. *Magn. Reson. Med.* **1991**, *17*, 164–178. (b) Lauffer, R. B. *Magn. Reson. Med.* **1991**, *22*, 339–342.
(28) Lauffer, R. B.; Parmelee, D. J.; Dunham, S. U.; Ouellet, H. S.; Dolan, R. P.; Witte, S.; McMurry, T. J.; Walovitch, R. C. *Radiology* **1998**, *207*, 529–538.
(29) Parmelee, D. J.; Walovitch, R. C.; Ouellet, H. S.; Lauffer, R. B. *Invest. Radiol.* **1997**, *32*, 741–747.

Scheme 1. Schematic Representation of the Synthesis of CB-TTDA[a]

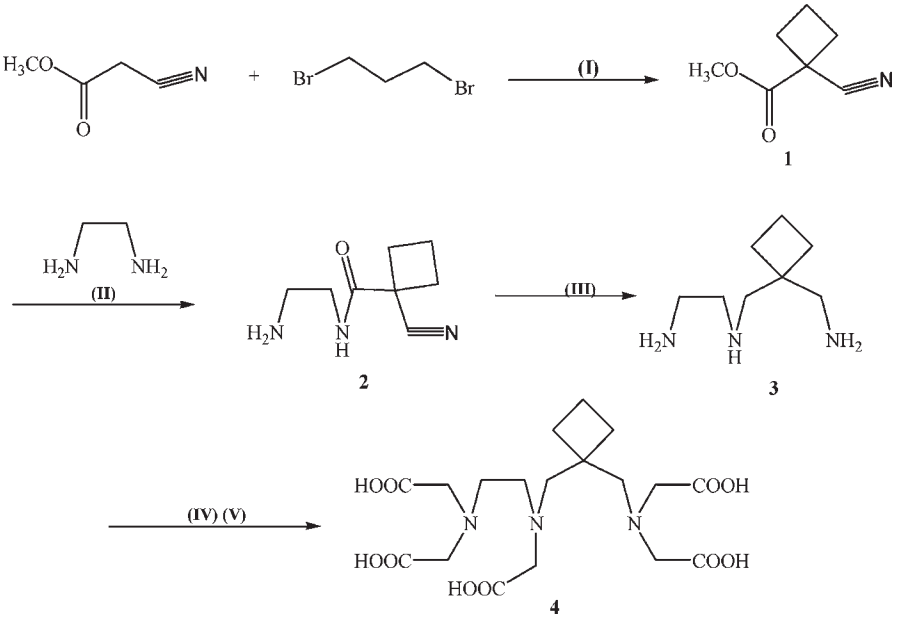

[a] (I) DBU, DMF; (II) MeOH; (III) BH_3-THF, THF; (IV) $BrCH_2COOt$-Bu, K_2CO_3, CH_3CN; and (V) HCl.

balanced modifications of the ligand carbon backbone with different structural moieties can affect not only its size, charge, and lipophilicity but also coordinating ability with Gd(III).[31] Furthermore, the presence of a hydrophobic residue will lead to a greater uptake in certain organs and may have potential to serve as organs specific agents.[32]

For the past few years, our group has been actively engaged in the development of $[Gd(TTDA)(H_2O)]^{2-}$ derivatives with the objective to study the effects of the substitution at different site of the TTDA on water exchange, rotational dynamics, and thermodynamic stability.[33,34] Here, we report the synthesis and physicochemical properties of two new TTDA derivatives, 6-carboxymethyl-3-{{[1-(*N*,*N*-dicarboxymethyl)-2-aminomethyl]-cyclobut-1-yl}methyl}-3,6-diazaoctanedioic acid (CB-TTDA) (Scheme 1) and 5-benzyl-6-carboxymethyl-3-{{[1-(*N*,*N*-dicarboxymethyl)-2′-aminomethyl]-cyclobut-1′-yl}-methyl}-3,6-diazaoctanedioic acid (Bz-CB-TTDA) (Scheme 2). The cyclobutyl[35] and benzyl[36] residues are introduced on the carbon backbone of $[Gd(TTDA)(H_2O)]^{2-}$ as a means to impart lipophilicity to the Gd(III) complexes. From our previous study, we have discovered that simply introducing the benzyl group on the carbon backbone of $[Gd(TTDA)(H_2O)]^{2-}$[36,37] was not enough to induce sufficient lipophilicity for angiographic application. Hence, apart from increasing the basicity of the ligand and the rigidity of Gd(III) complex, the primary intention for selecting the cyclobutyl is to tune the lipophilicity of $[Gd(Bz\text{-}CB\text{-}TTDA)(H_2O)]^{2-}$ to closely mimic that of MS-325. The ligand protonation constants and the thermodynamic and conditional stability constants of the ligands chelated with Gd(III), Cu(II), Zn(II), and Ca(II) and their selectivity for Gd(III) over endogenously available metal ions were estimated with the aim of assessing safety considerations for the two Gd(III) complexes as potential medical MRI CAs. The two key parameters affecting the proton relaxivity, water exchange and rotation dynamics, have been evaluated by combining variable temperature ^{17}O nuclear magnetic resonance (^{17}O NMR) and nuclear magnetic relaxation dispersion (NMRD) profile studies. Finally, the binding affinity of $[Gd(CB\text{-}TTDA)(H_2O)]^{2-}$ and $[Gd(Bz\text{-}CB\text{-}TTDA)(H_2O)]^{2-}$ toward HSA was evaluated by ultrafiltration and proton relaxation enhancement methods.

Materials and Methods

Chemicals. Reagents and solvents were purchased from commercial sources with the highest quality grade and were used without further purification, unless stated otherwise. ^{17}O-enriched water (20.3 atom %) was purchased from Isotec Inc. Human serum albumin (HSA, product no. A-1653, Fraction V Powder 96−99%) was purchased from Sigma and was used without any further purification,[38] and the molecular weight was assumed to be 69 kDa. The 50 mM phosphate buffer was used to maintain the pH of all solutions (pH 7.4) containing HSA. ^1H (400 MHz), ^{13}C (100 MHz), and ^{17}O (54.2 MHz) NMR spectra were recorded on a Varian Gemini-400 spectrometer with 5 mm sample tubes. Methyl cyanoacetate, ethylenediamine, BH_3·THF, cyclobutane-1,1-dicarboxylic acid diamide, L-phenylalanine, thionyl chloride, gadolinium chloride, and europium chloride were

(30) Caravan, P.; Comuzzi, C.; Crooks, W.; McMurry, T. J.; Choppin, G. R.; Woulfe, S. R. *Inorg. Chem.* **2001**, *40*, 2170–2176.
(31) (a) Artali, R.; Botta, M.; Cavallotti, C.; Giovenzana, G. B.; Palmisano, G.; Sisti, M. *Org. Biomol. Chem.* **2007**, *5*, 2441–2447. (b) Aime, S.; Geninatti Crich, S.; Gianolio, E.; Giovenzana, G. B.; Tei, L.; Terreno, E. *Coord. Chem. Rev.* **2006**, *250*, 1562–1579. (c) Aime, S.; Botta, M.; Terreno, E. *Adv. Inorg. Chem.* **2005**, *57*, 173–237. (d) Aime, S.; Botta, M.; Fasano, M.; Terreno, E. *Chem. Soc. Rev.* **1998**, *27*, 19–29.
(32) Sun, Y.; Martell, A. E.; Reibenspies, J. H.; Reichert, D. E.; Welch, M. J. *Inorg. Chem.* **2000**, *39*, 1480–1486.
(33) Wang, Y. M.; Li, C. R.; Huang, Y. C.; Ou, M. H.; Liu, G. C. *Inorg. Chem.* **2005**, *44*, 382–392.
(34) Ou, M. H.; Tu, C. H.; Tsai, S. C.; Lee, W. T.; Liu, G. C.; Wang, Y. M. *Inorg. Chem.* **2006**, *45*, 244–254.
(35) Liage, S. U.S. Patent 5905176, 1999.
(36) Hsu, J. S.; Jaw, T. S.; Liu, G. C.; Wang, Y. M.; Chen, S. H.; Kuo, Y. T.; Jao, J. C.; Li, C. W.; Tsai, K. *J. Magn. Reson. Imaging* **2004**, *20*, 632–639.
(37) Cheng, T. H.; Lee, T. M.; Ou, M. H.; Li, C. R.; Liu, G. C.; Wang, Y. M. *Helv. Chim. Acta* **2002**, *85*, 1033–1050.
(38) Cohn, E. J.; Strong, L. E.; Hughes, W. L., Jr.; Mulford, D. J.; Ashworth, J. N.; Melin, M.; Taylor, H. L. *J. Am. Chem. Soc.* **1946**, *68*, 459–475.

Scheme 2. Schematic Representation of the Synthesis of Bz-CB-TTDA[a]

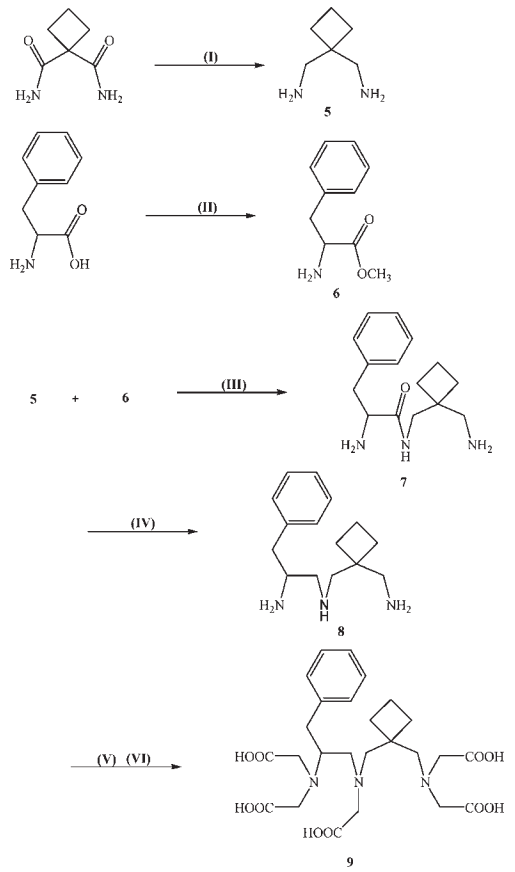

[a] (I) BH_3-THF, THF; (II) $SOCl_2$, MeOH; (III) TEA, MeOH; (IV) BH_3-THF, THF; (V) $BrCH_2COO$*t*-Bu, CH_3CN, K_2CO_3; and (VI) HCl.

purchased from Aldrich. 1,8-Diazabicyclo[5,4,0]undec-7-ene (DBU) and 1,3-dibromopropane were purchased from Alfa aesar. *tert*-Butyl bromoacetate was synthesized according to the reported procedure.[39] The details of the synthesis of CB-TTDA and Bz-CB-TTDA are reported in the Supporting Information, and refer to Schemes 1 and 2 for the formula.

Preparation of $[Ln(CB\text{-}TTDA)(H_2O)]^{2-}$ and $[Ln(Bz\text{-}CB\text{-}TTDA)(H_2O)]^{2-}$ Complexes. The Ln(III) = Eu(III) and Gd(III)) complexes were prepared by dissolving the ligand (0.05 mmol) in H_2O (3 mL), and the pH of the solution was adjusted to 6.5 with 1 M NaOH. To these solutions, 2.5 mL of an aqueous solution of $LnCl_3$ (0.05 mmol) was added dropwise, maintaining the pH at 6.5 with 1 M NaOH. The Ln(III) chelates were instantaneously formed at room temperature. For the ^{17}O NMR sample, $Gd(ClO_4)_3$ stock solution was prepared according to the literature.[33] The aqueous solutions of Gd(III) chelates were prepared by mixing the ligand and $Gd(ClO_4)_3$ stock solution in stoichiometric amounts. A slight ligand excess was used, and the pH of all solutions was adjusted using 1 M NaOH or $HClO_4$. The solutions were then evaporated under reduced pressure, and 1 equiv weight of 5.5% ^{17}O-enriched water was added. The absence of free metal in the solutions was checked by the xylenol orange test.[34]

Relaxation Time Measurement. Relaxation times T_1 of aqueous solutions of gadolinium(III) complexes were measured to determine relaxivity r_1. All measurements were made using a relaxometer operating at 20 MHz and 37.0 ± 0.1 °C (NMS 120 minispec, Bruker) by means of the standard inversion−recovery pulse sequence.

(39) Vollmar, A.; Dunn, M. S. *J. Org. Chem.* **1960**, *25*, 387–390.

Potentiometric Measurements. The protonation constants of the ligands were determined by potentiometric titrations of 1.0 mM ligand solutions using an automatic titrator system. To determine the stability constants for $[Gd(CB\text{-}TTDA)(H_2O)]^{2-}$ and $[Gd(Bz\text{-}CB\text{-}TTDA)(H_2O)]^{2-}$, competition titrations with EDTA were performed. The ratio of 1 Gd(III)/1 ligand/1 EDTA was employed. Under this condition, the metal ion is partitioned between ligand and EDTA, and the rate of transmetalation is fast enough between pH 2−4. However, complexation was usually rapid (3−5 min per point to give a stable pH reading) in the Cu(II), Ca(II), and Zn(II) studies. The same values of the stability constants were obtained by using the direct or back-titration. The autotitrating system consists of a 702 SM titroprocessor, a 728 stirrer, and a PT-100 combination pH electrode (Metrohm). The protonation constants of the ligands were calculated using a FORTRAN computer program, PKAS,[40] written for polyprotonic weak acid equilibria. The overall stability constants of the various metal complexes formed in aqueous solution were determined from the titration data with the FORTRAN computer program BEST.[40]

Variable-Temperature ^{17}O NMR Measurement. The measurement of the ^{17}O transverse relaxation rates, longitudinal relaxation rates, and chemical shifts was carried out with a Varian Gemini-400 spectrometer, equipped with a 10 mm probe, by using an external D_2O lock. The Varian 600 temperature control unit was used to stabilize the temperature in the range 278−338 K. Solutions containing 5.5% of the ^{17}O isotope were used. The inversion recovery sequence was applied to measure longitudinal relaxation rates, $1/T_1$, and the Carr−Purcell−Meiboom−Gill spin−echo technique was used to obtain transverse relaxation rates, $1/T_2$. The solution was introduced into spherical glass containers, fitting into ordinary 10 mm NMR tubes, in order to eliminate magnetic susceptibility corrections to chemical shifts.

Preparation of 4.5% (w/v) Human Serum Albumin (HSA) and GdL/HSA Solutions. HSA was dissolved in a 10 mM sodium phosphate and 150 mM sodium chloride (pH 7.4) solution. Two 4.5% (w/v) HSA solutions were prepared: one containing the GdL chelate at a concentration of 5.3 mM and another without the GdL chelate.

Ultrafiltration Measurements of Binding of GdL Chelate to HSA. GdL/HSA solutions ranging from 0.05 to 5.3 mM GdL chelate in 4.5% (w/v) HSA were made by combining appropriate amounts of 4.5% (w/v) HSA and 5.3 mM GdL in 4.5% (w/v) HSA solution. Aliquots (400 μL) of these solutions were placed in 30 kDa ultrafiltration units, incubated at 37.0 ± 0.1 °C for 20 min, and then centrifuged at 3500*g* for 10 min. The filtrates obtained from these ultrafiltration units were used to measure the concentration of free GdL chelate. Duplicate aliquots were operated for each sample. The Gd(III) concentrations of the GdL/HSA solutions and ultrafiltrates were obtained using ICP-MS.

Butanol Buffer Partition Coefficient. The Gd(III) chelated Bz-CB-TTDA ($[Gd]_T$ = 0.07 mM in 10 mL of PBS) was equilibrated at room temperature for 1−2 h with PBS-saturated butanol (10 mL). The vials were centrifuged at 2000*g* for 5 min to ensure that the layers were separated. Aliquots (5 mL) from each phase were removed and analyzed via inductively coupled plasma−atomic emission spectroscopy (ICP-AES, PerkinElmer OPTIMA 2000 PV). The partition coefficient (P) was calculated as follows.[41]

$$P = \frac{\text{avg conc of Gd(III) complex in butanol}}{\text{avg conc of Gd(III) complex in PBS}}$$

Transmetalation Experiments. This technique is based on measurement of the evolution of the water proton paramagnetic longitudinal relaxation rate (R_1^m) of a phosphate buffer solution

(40) Martell, A. E.; Motekaitis, R. J. *Determination and Use of Stability Constants*, 2nd ed.; VCH: New York, 1992.

(41) McMurry, T. J.; Parmelee, D. J.; Sajiki, H.; Scott, D. M.; Ouellet, H. S.; Walovitch, R. C.; Tyeklar, Z.; Dumas, S.; Bernard, P.; Nadler, S.; Midelfort, K.; Greenfield, M.; Troughton, J.; Lauffer, R. B. *J. Med. Chem.* **2002**, *45*, 3465–3474.

Table 1. Protonation Constants of Bz-CB-TTDA, CB-TTDA, TTDA, MS-325, EPTPA-bz-NO_2, and DTPA at I = 0.1 M Me_4NCl[a] and T = 25.0 ± 0.1 °C

	log K_i					
equilibrium	Bz-CB-TTDA	CB-TTDA	TTDA[a]	MS-325[b]	EPTPA-bz-NO_2[c]	DTPA[d]
[HL]/[L][H]	10.72 (0.04)	11.08 (0.03)	10.60	11.15 (0.12)	10.86	10.49
$[H_2L]/[HL][H]$	9.40 (0.01)	9.17 (0.05)	8.92	8.62 (0.06)	8.91	8.60
$[H_3L]/[H_2L][H]$	5.54 (0.09)	5.23 (0.02)	5.12	4.51 (0.09)	4.70	4.28
$[H_4L]/[H_3L][H]$	2.43 (0.03)	3.11 (0.04)	2.80	2.96 (0.06)	3.25	2.64
ΣpK_a	28.09	28.59	27.44	27.24	27.72	26.01

[a] Data were obtained from ref 33. [b] Data were obtained from ref 30. [c] Data were obtained from ref 44. [d] Data were obtained from ref 45.

containing 2.5 mM Gd(III) complex and 2.5 mM $ZnCl_2$.[42,43] Relaxation rate (R_1^m) measurements were performed at 37.0 ± 0.1 °C and 20 MHz (Bruker Minispec 120).

Data Analysis. The simultaneous least-squares fitting of ^{17}O NMR data and the binding parameters to HSA were determined by fitting the experimental data using the program SCIENTIST for Windows by MICROMATH, version 2.0.

Results and Discussion

Synthesis of $[Gd(CB\text{-}TTDA)(H_2O)]^{2-}$. The ligand CB-TTDA was synthesized in four steps, as shown in Scheme 1 (the detailed synthesis method is summarized in the Supporting Information). In the first step methyl cyanoacetate was treated with 1,3-dibromopropane in the presence of DBU in DMF at 70 °C. The compound 1-cyano-cyclobutanecarboxylic methyl ester (**1**) was obtained. Subsequently, compound **1** was reacted with ethylenediamine in methanol at room temperature for 15 h. It gave rise to 1-cyano-cyclobutanecarboxylic acid (2-aminoethyl) amide (**2**). The solution of **2** and $BH_3 \cdot THF$ was stirred for 15 h at 60 °C, followed by the addition of the 6 M HCl resulted in the formation of compound **3**. Finally, compound **3** was treated with *tert*-butylbromoacetate in the presence of anhydrous K_2CO_3 in CH_3CN at 80 °C to provide CB-TTDA(**4**). $[Gd(CB\text{-}TTDA)(H_2O)]^{2-}$ identified by LC-MS was obtained by complexation of Gd(III) with CB-TTDA in water at room temperature.

Synthesis of $[Gd(Bz\text{-}CB\text{-}TTDA)(H_2O)]^{2-}$. The synthetic scheme of Bz-CB-TTDA ligand is depicted in Scheme 2 (the detail synthesis method is summarized in the Supporting Information). The synthesis procedure begins with reduction of amide in cyclobutane-1,1-dicarboxylic acid diamide with $BH_3 \cdot THF$ in THF at 60 °C to obtain (1-(aminomethyl)cyclobutyl)methamine (**5**). Subsequently, compound **5** was treated with L-phenylalanine methyl ester in methanol at room temperature for 15 h to obtain 2-amino-*N*-((1-aminomethyl)cyclobutyl)-3-phenylpropanamide (**7**). Finally, treatment of compound **8** with *tert*-butylbromoacetate in the presence of anhydrous K_2CO_3 in CH_3CN at 90 °C provides Bz-CB-TTDA (**9**) which was characterized by ^1H NMR and LC-MS. $[Gd(Bz\text{-}CB\text{-}TTDA)(H_2O)]^{2-}$ identified by LC-MS was obtained by complexation of Gd(III) with Bz-CB-TTDA in water at room temperature.

Protonation and Stability Constant. The potentiometric titration curves for Bz-CB-TTDA and CB-TTDA have been deposited as Supporting Information (Figures 5S and 6S in the Supporting Information). The protonation constants (log K_i) of Bz-CB-TTDA and CB-TTDA, which were calculated from potentiometric titration curves, are reported in Table 1 along with those of TTDA, MS-325 (4-(*R*)-[(4,4-diphenyl-cyclohexyl)-phosphanooxyethyl]3,6,9-triaza-3,6,9-tris(methoxy-carbonyl)-undecanedioato gadolinium(III)) ligand, EPTPA-bz-NO_2 ((4-*p*-nitrobenzyl-3,6,10-tri(carboxymethyl)-3,6,10-triazadodecanedioic acid),[44] and DTPA (3,6,9-tri(carboxymethyl)-3,6,9-triazaundecanedioic acid)[45] (Chart 1). The overall basicity of each ligand can be quantified by calculating ΣpK_a.[46] A comparison of the ΣpK_a values of CB-TTDA (28.59) and Bz-CB-TTDA (28.09) to that of its parent TTDA (27.44) indicates that the introduction of the four member ring on the carbon backbone of TTDA significantly increases the ΣpK_a value. This result implies that the presence of cyclobutyl in CB-TTDA and Bz-CB-TTDA considerably increases their basicity. The overall basicity decreases in the following order: CB-TTDA > Bz-CB-TTDA ≈ EPTPA-bz-NO_2 ≈ TTDA ≈ MS-325 > DTPA.

All of the metal complexes show titration curve depression (Figures 5S and 6S in the Supporting Information) relative to the titration curve for the ligand, reflecting complex formation. The thermodynamic stability of a metal complex is given by the thermodynamic stability constants ($K_{ML(therm)}$), following eq 1

$$K_{ML(therm)} = \frac{[ML]}{[M][L]} \quad (1)$$

where [M], [L], and [ML] are the concentrations of the metal ion, the deprotonated ligand, and the complex, respectively. The thermodynamic stability constants of CB-TTDA, Bz-CB-TTDA, TTDA, EPTPA-bz-NO_2, and DTPA complexes with different metal ions are summarized in Table 2. The order of increase in the stability constant for these ligands chelated with Gd(III) is $[Gd(TTDA)(H_2O)]^{2-} \approx [Gd(EPTPA\text{-}bz\text{-}NO_2)(H_2O)]^{2-} < [Gd(CB\text{-}TTDA)(H_2O)]^{2-} \approx [Gd(Bz\text{-}CB\text{-}TTDA)(H_2O)]^{2-} < [Gd(DTPA)(H_2O)]^{2-} \approx$ MS-325. The higher stability constants of the CB-TTDA and Bz-CB-TTDA with Gd(III), Ca(II), Cu(II), and Zn(II) compared to those of TTDA and EPTPA-bz-NO_2 can be explained in terms of steric effect and basicity. The stability of Gd(III) complexes is influenced by their coordination geometry which is dictated by the ligand structure and flexibility.[47] The

(42) Laurent, S.; Vander Elst, L.; Muller, R. N. *Contrast Media Mol. Imaging* **2006**, *1*, 128–137.
(43) Laurent, S.; Vander Elst, L.; Copoix, F.; Muller, R. N. *Invest. Radiol.* **2001**, *36*, 115–122.
(44) Laus, S.; Ruloff, R.; Tóth, E.; Merbach, A. E. *Chem.—Eur. J.* **2003**, *9*, 3555–3566.
(45) Smith, R. M.; Martell, A. E. *Critical Stability Constants*; Plenum: New York, 1974.
(46) Kumar, K.; Tweedle, M. F.; Malley, M. F.; Gougoutas, J. Z. *Inorg. Chem.* **1995**, *34*, 6472–6480.
(47) Tei, L.; Baranyai, Z.; Botta, M.; Piscopo, L.; Aime, S.; Giovenzana, G. B. *Org. Biomol. Chem.* **2008**, *6*, 2361–2368.
(48) Rabasso, N.; Louaisil, N.; Fadel, A. *Tetrahedron.* **2006**, *62*, 7445–7454.

Chart 1

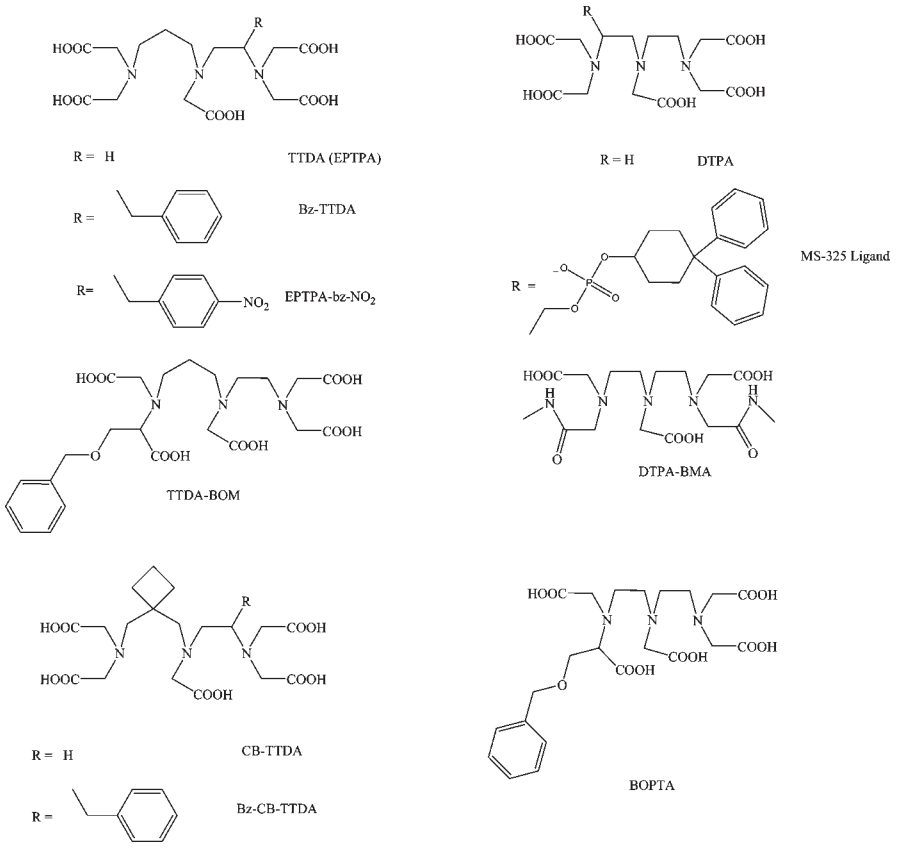

Table 2. Stability Constants, Conditional Stability Constants, Selectivity Constants, and Modified Selectivity Constants of Gd^{3+}, Zn^{2+}, Ca^{2+}, and Cu^{2+} Complexes with Bz-CB-TTDA, CB-TTDA, TTDA, MS-325, EPTPA-bz-NO_2, and DTPA at I = 0.1 M Me_4NCl; T = 25.0 ± 0.1 °C[a]

parameter	Bz-CB-TTDA	CB-TTDA	TTDA[b]	MS-325[c]	EPTPA-bz-NO_2[d]	DTPA[e]
log $K_{GdL(therm)}$	20.09 (0.04)	20.28 (0.03)	18.96	22.06 (0.02)	19.20	22.46
log $K_{GdL(cond)}$ (pH = 7.4)	14.77	14.82	14.25	17.06	14.22	18.14
pGd	15.77	15.82	15.25	19.94	15.3	19.14
log $K_{caL(therm)}$	9.32 (0.04)	9.52 (0.02)	9.13	10.45 (0.06)	9.38	10.75
log K_{CaHL}	6.31 (0.05)	6.24 (0.02)	8.20	5.66 (0.02)		6.11
log $K_{CaL(cond)}$ (pH = 7.4)	4.00	4.06	4.42	5.45	4.40	6.43
pCa	5.03	5.09	6.28	8.34		7.46
log $K_{ZaL(therm)}$	15.97 (0.06)	16.06 (0.03)	16.03	17.82 (0.09)	16.01	18.70
log K_{ZnHL}	8.29 (0.02)	8.13 (0.04)	7.80	5.60 (0.02)		5.60
log $K_{ZnL(cond)}$ (pH = 7.4)	10.65	10.60	11.32	12.82	11.03	14.38
pZn	12.58	12.41	12.86	15.71		15.39
log $K_{CuL(therm)}$	17.26 (0.04)	17.71 (0.02)	16.77	21.3 (0.3)	18.47	21.38
log K_{CuHL}	7.20 (0.06)	5.29 (0.03)	5.69	5.16 (0.08)		4.81
log $K_{CuL(cond)}$ (pH = 7.4)	11.94	12.25	12.06	16.30	13.49	17.00
pCu	13.15	13.26	13.06	19.18		18.06
log K_{sel}(Gd/Ca)	10.77	10.76	9.83	11.61	9.82	11.71
log K_{sel}(Gd/Zn)	4.12	4.22	2.93	4.24	3.19	3.76
log K_{sel}(Gd/Cu)	2.83	2.57	2.19	0.76	0.73	1.08
log $K_{sel'}$	8.28	8.24	7.18	6.75	6.65	7.06

[a] Uncertainty (σ) in log K values are given in parentheses. [b] Data were obtained from ref 33. [c] Data were obtained from ref 30. [d] Data were obtained from ref 44. [e] Data were obtained from ref 45.

cyclobutyl residue on the carbon backbone of TTDA may increase the steric rigidity.[48] This could facilitate the CB-TTDA and the Bz-CB-TTDA to constrain into a chelating conformation, consequently escalating their coordinating ability toward metal ion. A fraction of this increase in stability is also due to higher basicity[49] of CB-TTDA and Bz-CB-TTDA than those of TTDA and EPTPA-bz-NO_2.

(49) Kumar, K.; Tweedle, M. F. *Inorg. Chem.* **1993**, *32*, 4193–4199.

Conditional Stability and Selectivity Constant. Several studies have emphasized the importance of the conditional stability constant for evaluating the stability of Gd(III) complex under physiological pH 7.4. The conditional stability constant can be calculated by using eq 2

$$K_{ML(therm)} = K_{ML(cond)}\left(1 + K_1[H^+] + K_1K_2[H^+]^2 + \cdots + K_n[H^+]^n\right) \quad (2)$$

where K_1, K_2, K_3 ,..., K_n are the stepwise protonation constant of the ligand. The conditional stability constants of CB-TTDA, Bz-CB-TTDA, TTDA, EPTPA-bz-NO_2, and DTPA complexed with different metals ions (Gd(III), Zn(II), Cu(II)) are given in Table 2. It is smaller than that of thermodynamic stability constant due to the competition between H^+ and the metal ion for the ligand at physiological pH. Moreover, very significant information on the stability of the metal complex and sequestering ability of the ligand at physiological condition comes from the pM value ($pM = -\log[M_f]$, where $[M_f]$ is the equibilirum concentration of the free aqua metal ion present at pH = 7.4). The pM values reflect the influence of the ligand basicity and the protonation of the complex. The larger the pM value is, the higher is the affinity of the ligand for the metal ion under the given condition; that is, the larger the pM is, the lower the concentration of free metal ion present.[44,50] The pM values of CB-TTDA, Bz-CB-TTDA, TTDA, EPTPA-bz-NO_2, and DTPA with different metal ions (Gd(III), Ca(II), Cu(II), and Zn(II)) are summarized in Table 2. The pGd values of $[Gd(CB\text{-}TTDA)(H_2O)]^{2-}$ and $[Gd(Bz\text{-}CB\text{-}TTDA)(H_2O)]^{2-}$ are higher than those of their pCa, pZn, and pCu values. There is only a small difference between the pGd and the pCu values of CB-TTDA and Bz-CB-TTDA; hence, Cu(II) can compete with Gd(III) for these ligands from a thermodynamic viewpoint. However, Cu(II) exists in very low concentrations in vivo. The metal ions, Zn(II) and Ca(II), have lower affinity for CB-TTDA and Bz-CB-TTDA than that of Gd(III) at pH 7.4. The pGd values of $[Gd(CB\text{-}TTDA)(H_2O)]^{2-}$ and $[Gd(Bz\text{-}CB\text{-}TTDA)(H_2O)]^{2-}$ are slightly higher than those of $[Gd(TTDA)(H_2O)]^{2-}$ and $[Gd(EPTPA\text{-}bz\text{-}NO_2)(H_2O)]^{2-}$ due to elevated basicity and rigidity endowed by cyclobutyl groups. However, both complexes, $[Gd(CB\text{-}TTDA)(H_2O)]^{2-}$ and $[Gd(Bz\text{-}CB\text{-}TTDA)(H_2O)]^{2-}$, have lower pGd values than those of $[Gd(DTPA)H_2O]^{2-}$ and MS-325. Furthermore, as the blood pool agent retains in the bloodstream for longer time, reactions of CAs with various endogenous substances (metal ions and biological ligands) may occur. Evaluation of competition between Gd(III) and the endogenous metal ions must be taken into account for toxicological reasons. The logarithmic selectivity constants (defined as $\log(K_{GdL}/K_{ML})$, M = Zn(II), Ca(II), and Cu(II)) of CB-TTDA, Bz-CB-TTDA, TTDA, EPTPA-bz-NO_2, and DTPA for Gd(III) over Ca(II), Zn(II), and Cu(II) are summarized in Table 2. The selectivity of both CB-TTDA and Bz-CB-TTDA for Gd(III) against Zn(II) is higher than those of TTDA, EPTPA-bz-NO_2, and DTPA, but is smaller than that of MS-325. Higher selectivity toward Gd(III) against Zn(II) indicates that endogenously available Zn(II) ion, which is one of the most copious metal ions in blood plasma, is less able to displace Gd(III) in the chelate. Additionally, the modified selectivity constant ($\log K_{sel'}$) given by eq 3[46] provides more precise information about the selectivity for Gd(III) over other endogenous metal ions and H^+ for a ligand

$$K_{sel'} = K_{ML(therm)}\left(\alpha_H{}^{-1} + \alpha_{CaL}{}^{-1} + \alpha_{CuL}{}^{-1} + \alpha_{ZnL}{}^{-1}\right)^{-1} \quad (3)$$

where α is a side reaction coefficient (eqs 1S−4S in the Supporting Information). $\log K_{sel'}$ is a thermodynamic stability constant corrected for the competition between the endogenously available metal ions and H^+. The calculated $\log K_{sel'}$ values for the Gd(III) complexes are summarized in Table 2 and follow the order CB-TTDA (8.24) ∼ Bz-CB-TTDA (8.28) > TTDA (7.18) ∼ DTPA (7.06) > MS-325 (6.75) > EPTPA-bz-NO_2 (6.65). These results imply that $[Gd(CB\text{-}TTDA)(H_2O)]^{2-}$ and $[Gd(Bz\text{-}CB\text{-}TTDA)(H_2O)]^{2-}$ are fairly stable under physiological conditions.

Assessment of the Hydration State. Luminescence lifetime measurements have been used to quantify the number of inner-sphere water molecules[51] in $[Gd(Bz\text{-}CB\text{-}TTDA)(H_2O)]^{2-}$ and $[Gd(CB\text{-}TTDA)(H_2O)]^{2-}$. Eu(III) is commonly applied for lifetime measurements because it emits in the visible region and shows longer emission lifetime.[52] In the lanthanide series of the periodic table, Gd(III) ($Z = 64$) just comes after Eu(III) ($Z = 63$), and hence, Gd(III) has nearly the same ratio of charge to ionic radius as Eu(III) and correspondingly similar coordination chemistry. Therefore, the number of inner-sphere water molecules determined for $[Eu(Bz\text{-}CB\text{-}TTDA)(H_2O)]^{2-}$ and $[Eu(CB\text{-}TTDA)(H_2O)]^{2-}$ should correspond to the hydration status of Gd(III) complexes of these ligands. The emission lifetimes (τ) of the Eu($^5D_0$) excited level have been measured in 2 mM solutions of the $[Eu(Bz\text{-}CB\text{-}TTDA)(H_2O)]^{2-}$ and $[Eu(CB\text{-}TTDA)(H_2O)]^{2-}$ in D_2O and H_2O, and were used to calculate the number of coordinated water molecules q (Table 3) using eqs 4 and 5[53]

$$q = 1.05\left[\tau_{H_2O}{}^{-1} + \tau_{D_2O}{}^{-1}\right] \quad (4)$$

$$q = 1.2\left[\left(\tau_{H_2O}{}^{-1} + \tau_{D_2O}{}^{-1}\right) - 0.25\right] \quad (5)$$

where q is the number of water molecules bound to metal ions, τ_{H_2O} is the luminescence half-life in H_2O solution, and τ_{D_2O} is the luminescence half-life in D_2O solution. Equation 5 takes into account the vibration of the N−H bonds. Consequently, eq 5 is a little more precise than eq 4. The q values obtained for $[Eu(Bz\text{-}CB\text{-}TTDA)(H_2O)]^{2-}$ and $[Eu(CB\text{-}TTDA)(H_2O)]^{2-}$ fall within the usual range that corresponds to single hydration. For instance, the q values of $[Eu(Bz\text{-}CB\text{-}TTDA)(H_2O)]^{2-}$ and $[Eu(CB\text{-}TTDA)(H_2O)]^{2-}$ are similar to those of MS-325,[16] $[Eu(BOPTA)(H_2O)]^{2-}$ (BOPTA = 4-carboxy-5,8,11-tris(carboxymethyl)-1-phenyl-2-oxa-5,8,11-triazatridecan-13-oic acid),[54] and $[Eu(DTPA)(H_2O)]^{2-}$[55] (Chart 1). Hence, a general

(50) (a) Bannochie, C. J.; Martell, A. E. *Inorg. Chem.* **1991**, *30*, 1385–1392. (b) Tweedle, M. F.; Hahan, J. J.; Kumar, K.; Mantha, S.; Chang, C. A. *Magn. Reson. Imaging* **1991**, *9*, 409–415.

(51) Horrocks, W. D., Jr.; Sudnick, D. R. *Acc. Chem. Res.* **1981**, *14*, 384–392.

(52) Mato-Iglesias, M.; Roca-Sabio, A.; Pálinkás, Z.; Esteban-Gómez, D.; Platas-Iglesias, C.; Tóth, E.; de Blas, A.; Rodríguez-Blas, T. *Inorg. Chem.* **2008**, *47*, 7840–7851.

(53) (a) Beeby, A.; Clarkson, I. M.; Dickins, R. S.; Faulkner, S.; Parker, D.; Royle, L.; Sousa, A. S. d.; Williams, J. A. G.; Woods, M. *J. Chem. Soc., Perkin Trans.* **1999**, *2*, 493–504. (b) Horrocks, W. D.; Sudnick, D. R. *J. Am. Chem. Soc.* **1979**, *101*, 334–340.

(54) Anelli, P. L.; Balzani, V.; Prodi, L.; Uggeri, F. *Gazz. Chim. Ital.* **1991**, *121*, 359–364.

(55) Bryden, C. C.; Reilley, C. N. *Anal. Chem.* **1982**, *54*, 610–615.

Table 3. Luminescence Lifetimes of $[Eu(CB\text{-}TTDA)(H_2O)]^{2-}$, $[Eu(Bz\text{-}CB\text{-}TTDA)(H_2O)]^{2-}$, MS-325, $[Eu(BOPTA)(H_2O)]^{2-}$, and $[Eu(DTPA)(H_2O)]^{2-}$ Complexes and Number of Inner-Sphere Water Molecules (q)

	luminescence lifetimes		q	
Eu(III) complex	τ_{H_2O} (ms)	τ_{D_2O} (ms)	eq *4*	eq *5*
$[Eu(CB\text{-}TTDA)(H_2O)]^{2-}$[a]	0.64	2.44	1.21 ± 0.01	1.09 ± 0.02
$[Eu(Bz\text{-}CB\text{-}TTDA)(H_2O)]^{2-}$[a]	0.62	2.49	1.26 ± 0.02	1.41 ± 0.03
MS-325[b]				1.02
$[Eu(BOPTA)(H_2O)]^{2-}$[c]			1.2	
$[Eu(DTPA)(H_2O)]^{2-}$[d]			1.2	

[a] The value was determined with eqs 4 and 5. [b] Data were obtained from ref 16. [c] Data were obtained from ref 54. [d] Data were obtained from ref 55. Reported errors are statistical errors, but the methodological errors are much larger.

formula of $[Eu(L)(H_2O)]^{2-}$ can be proposed for these complexes in solution.

Relaxometric Studies of Gd(III) Complexes. The longitudinal water proton relaxivity (r_1) that results from the contribution of the water molecules in the inner and outer coordination spheres is given by eq 6.[56]

$$r_1 = r_1^{IS} + r_1^{OS} \quad (6)$$

The superscripts "IS" and "OS" refer to the inner and outer sphere, respectively. It is exceedingly difficult to alter the outer-sphere contribution.[57] Furthermore, for the Gd(III) complexes of similar size, it can be assumed that the outer sphere makes a similar contribution at high magnetic flux density (>0.1 T). Consequently, for the new generation contrast agent of higher efficiency, the inner-sphere contribution becomes much more important and is expressed by eq 7[57−59]

$$r_1^{IS} = \frac{qC}{55.6}\frac{1}{T_{1M} + \tau_M} \quad (7)$$

where C represents the molar concentration of the Gd(III) complex, q is the number of water molecules bound to metal ions, T_{1M} is the longitudinal relaxation time of the inner-sphere water protons, and τ_M is the residence lifetime of the bound water. Thus, r_1^{IS} is maximized when $T_{1M} > \tau_M$ (fast exchange conditions) and T_{1M} is as short as possible.[59] The longitudinal relaxivity (r_1) values of $[Gd(Bz\text{-}CB\text{-}TTDA)(H_2O)]^{2-}$ and $[Gd(CB\text{-}TTDA)(H_2O)]^{2-}$ determined at 20 MHz and 37.0 ± 0.1 °C are shown in Table 4 and Figure 8S in the Supporting Information along with those of $[Gd(TTDA)(H_2O)]^{2-}$[9] and $[Gd(DTPA)(H_2O)]^{2-}$.[60] The relaxivity of $[Gd(Bz\text{-}CB\text{-}TTDA)(H_2O)]^{2-}$ is similar to that of $[Gd(CB\text{-}TTDA)(H_2O)]^{2-}$ and slightly higher than those of $[Gd(TTDA)(H_2O)]^{2-}$ and $[Gd(DTPA)(H_2O)]^{2-}$ owing to higher molecular weight. Although the water exchange rate on $[Gd(TTDA)(H_2O)]^{2-}$ is much higher than that of $[Gd(DTPA)(H_2O)]^{2-}$, the relaxivity profile shown by the two complexes is similar.[9,33] This is due to the fact that the relaxivity of the low molecular weight Gd(III) complexes is limited by rotational correlation time rather than water exchange rate. As a consequence, the difference in water exchange rate in the two Gd(III) complexes has practically no influence on the relaxivity which is restricted by fast rotation.

Table 4. Relaxivity r_1 of $[Gd(CB\text{-}TTDA)(H_2O)]^{2-}$, $[Gd(Bz\text{-}CB\text{-}TTDA)(H_2O)]^{2-}$, MS-325 $[Gd(TTDA)(H_2O)]^{2-}$, and $[Gd(DTPA)(H_2O)]^{2-}$ at 37.0 ± 0.1°C and 20 MHz

complex	pH	relaxivity r_1 ($mM^{-1}\ s^{-1}$)
$[Gd(CB\text{-}TTDA)(H_2O)]^{2-}$	7.4 ± 0.1	4.12 ± 0.05
$[Gd(Bz\text{-}CB\text{-}TTDA)(H_2O)]^{2-}$	7.4 ± 0.1	4.29 ± 0.03
MS-325[a]	7.4 ± 0.1	6.84 ± 0.48
$[Gd(TTDA)(H_2O)]^{2-}$[b]	7.5 ± 0.1	3.85 ± 0.03
$[Gd(DTPA)(H_2O)]^{2-}$[c]	7.6 ± 0.1	3.89 ± 0.03

[a] Data were obtained from ref 59. [b] Data were obtained from ref 9. [c] Data were obtained from ref 60

Water-Exchange Rate and Rotational Correlation Time Studies of Gd(III) Complexes. To probe the microscopic parameters that determine the proton relaxivity of a Gd(III) complex, for instance, the water exchange rate (k_{ex}), the rotational correlation time (τ_R), and the electron spin relaxation ($1/T_{1,2e}$), and to better understand the consequence of structural modification of ligand on the water exchange and the rotational dynamics, we carried out a combined NMRD and variable temperature ^{17}O NMR study. The former technique measures the excess longitudinal proton relaxation caused by the presence of the Gd(III) complex as a function of magnetic field.[61] The method is a direct measure of relaxation rate and is theoretically sensitive to all the parameters that influence relaxation rate. However, there are many parameters that are ill-defined by the NMRD curve alone.[12] Combination of ^{17}O NMR is helpful to investigate the number of parameters that influence proton relaxivity, for instance, the number of inner-sphere water molecules, the rotational correlation time, and the longitudinal electronic relaxation rate of the complexes.[62−64] In addition, it is an efficient technique to study water exchange rate and its mechanism of reaction which can be elucidated by

(56) Tóth, E., Helm, L., Merbach, A. E., Eds. *The Chemistry of Contrast Agents in Medical Magnetic Resonance Imaging*; John Wiley and Sons: New York, 2001; pp 45−119.
(57) Swift, T. J.; Connick, R. E. *J. Chem. Phys.* **1962**, *37*, 307–320.
(58) Luz, Z.; Meiboom, S. *J. Chem. Phys.* **1964**, *40*, 1058–1066.
(59) (a) Caravan, P.; Parigi, G.; Chasse, J. M.; Cloutier, N. J.; Ellison, J. J.; Lauffer, R. B.; Luchinat, C.; McDermid, S. A.; Spiller, M.; McMurry, T. J. *Inorg. Chem.* **2007**, *46*, 6632–6639. (b) Aime, S.; Botta, M.; Fasano, M.; Terreno, E. *Acc. Chem. Res.* **1999**, *32*, 941–949.
(60) Weinmann, H. J.; Brasch, R. C.; Press, W. R.; Wesbey, G. E. *Am. J. Roentgenol.* **1984**, *142*, 619–624.
(61) Koenig, S. H.; Brown, R. D., III. *Prog. NMR Spectrosc.* **1990**, *22*, 487–567.
(62) Gonzalez, G.; Powell, D. H.; Tissiéres, V.; Merbach, A. E. *J. Phys. Chem.* **1994**, *98*, 53–59.
(63) Micskei, K.; Helm, L.; Brücher, E.; Merbach, A. E. *Inorg. Chem.* **1993**, *32*, 3844–3850.
(64) Micskei, K.; Powell, D. H.; Helm, L.; Brücher, E.; Merbach, A. E. *Magn. Reson. Chem.* **1993**, *31*, 1011–1020.
(65) Frey, U.; Merbach, A. E.; Powell, D. H In *Solvent Exchange on Metal Ions: A Variable NMR Approach*; Delpuech, J.-J., Ed.; John Wiley & Sons: Chichester, U.K., 1995; p 263.

variable pressure measurement.[65,66] The main advantage of the ^{17}O NMR technique is that the outer-sphere contributions to both transverse and longitudinal ^{17}O relaxation rates are negligible; this is due to the fact that the oxygen nucleus is closer to the paramagnetic center when it is bound in the inner sphere.[63] Since the oxygen is directly coordinated to Gd(III), the scalar contribution is the most significant in the case of the ^{17}O transverse relaxation.[63] Furthermore, the longitudinal relaxation rates in Gd(III) complex solutions are dominated by dipole−dipole and quadrupolar interactions and give direct access to the rotational correlation time of the Gd−O vector (τ_R).[67] The ^{17}O NMR and NMRD data for $[Gd(CB\text{-}TTDA)(H_2O)]^{2-}$ and $[Gd(Bz\text{-}CB\text{-}TTDA)(H_2O)]^{2-}$ have been analyzed simultaneously (all the relevant equations are given in the Supporting Information) and are shown together with fitted curves in Figure 1. In order to reduce the number of variables in the fit, some of the parameters were set to fixed values or adopted from the data published for $[Gd(TTDA)(H_2O)]^{2-}$ derivatives.[33,34,44] The parameters affecting water exchange and proton relaxivity of $[Gd(CB\text{-}TTDA)(H_2O)]^{2-}$ and $[Gd(Bz\text{-}CB\text{-}TTDA(H_2O)]^{2-}$ are summarized and compared with other Gd(III) complexes in Table 5.

The k_{ex} value can be directly computed from variable temperature transverse ^{17}O relaxation rates measured for Gd(III) complex solutions. The reduced relaxation rates and the chemical shift, $1/T_{1r}$, $1/T_{2r}$, and $\Delta\omega_r$ can be calculated from measured ^{17}O NMR relaxation rates and angular frequency of the paramagnetic solution $1/T_1$, $1/T_2$, and ω, and the acidified water reference $1/T_{1A}$, $1/T_{2A}$, and ω_A. The data fitted simultaneously according to eqs 5S−13S[68−70] can be found in the Supporting Information.

The maxima on the reduced transverse ^{17}O relaxation rate ($1/T_{2r}$) curve and the inflection point on the reduced chemical shift ($\Delta\omega_r$) curve indicates the change over from the fast exchange domain to the slow exchange.[56] However, in the case of $[Gd(CB\text{-}TTDA)(H_2O)]^{2-}$ and $[Gd(Bz\text{-}CB\text{-}TTDA)(H_2O)]^{2-}$ over the whole temperature range, we observed neither maxima nor inflection on $1/T_{2r}$ and $\Delta\omega_r$ curves; that is, the $1/\tau_m$ side of the curve is not observed (Figure 1).[71] These results indicate that the system is in the fast exchange domain ($k_{ex} \gg 1/T_{2m}$) and the slow exchange region does not exist over the studied temperature range.[71] Consequently, $1/T_{2r}$ is determined by the relaxation rate of the coordinated water molecule ($1/T_{2m}$), which is influenced by the water residence time ($\tau_m = 1/k_{ex}$), the longitudinal electronic relaxation rate ($1/T_{1e}$), and the scalar coupling constant ($A/\hbar$).[34]

The k_{ex}^{298} values for $[Gd(CB\text{-}TTDA)(H_2O)]^{2-}$ and $[Gd(Bz\text{-}CB\text{-}TTDA)(H_2O)]^{2-}$ along with other structurally related Gd(III) complexes are summarized in Table 5. The k_{ex}^{298} values for $[Gd(CB\text{-}TTDA)(H_2O)]^{2-}$ and $[Gd(Bz\text{-}CB\text{-}TTDA)(H_2O)]^{2-}$ are significantly higher than those of clinically used nine-coordinate Gd(III) complexes, for instance, $[Gd(DTPA)(H_2O)]^{2-}$, $[Gd(DTPA\text{-}BMA)(H_2O)]$, and $[Gd(DOTA)(H_2O)]^{-}$. The high water exchange rate on $[Gd(CB\text{-}TTDA)(H_2O)]^{2-}$ and $[Gd(Bz\text{-}CB\text{-}TTDA)(H_2O)]^{2-}$ can be explained in terms of carbon backbone length. The longer carbon backbone of CB-TTDA and Bz-CB-TTDA compared to that of DTPA facilitates better wrapping of the Gd(III) ion and is pulled tightly into the first coordination sphere.[44] This leads to crowding on the water binding site, which in turn facilitates in squeezing out the bonded water molecules. The water exchange rate is further accelerated due to the rigidity endowed by the presence of the cyclobutyl group[49] on the carbon backbone of $[Gd(CB\text{-}TTDA)(H_2O)]^{2-}$ and $[Gd(Bz\text{-}CB\text{-}TTDA)(H_2O)]^{2-}$. The water exchange on $[Gd(CB\text{-}TTDA)(H_2O)]^{2-}$ and $[Gd(Bz\text{-}CB\text{-}TTDA)(H_2O)]^{2-}$ most probably takes place via a limiting dissociative D mechanism based on the structural analogy to $[Gd(EPTPA)(H_2O)]^{2-}$ (EPTPA = 3,6,10-tri(carboxymethyl)-3,6,10-triazadodecanedioic acid).[44]

The rotational correlation time (τ_R) is a vital parameter that influences proton relaxivity. NMRD technique has been frequently employed for the determination of τ_R values. A negligible scalar relaxation contribution simplifies the treatment of NMRD data. The τ_R value of a Gd(III) complex can also be determined from the longitudional ^{17}O relaxation (transverse relaxation contains no information on rotational motion of the system). A major drawback of both techniques is reliability on distance estimation (Gd−H distance for ^{1}H-NMRD and Gd−O distance for ^{17}O NMR). Furthermore, discrepancy in the τ_R value obtained from NMRD and ^{17}O NMR has been observed, and the τ_R value obtained by NMRD is generally lower than that of ^{17}O NMR. Due to the practical importance of NMRD data for MRI, contrast agents are generally characterized by the τ_R value obtained from NMRD.[72] The τ_R^{298} values for $[Gd(CB\text{-}TTDA)(H_2O)]^{2-}$ and $[Gd(Bz\text{-}CB\text{-}TTDA)(H_2O)]^{2-}$ obtained by fitting ^{17}O NMR and NMRD data are shown in Table 5. The order of τ_R^{298} values obtained by fitting ^{17}O NMR and NMRD data is $[Gd(Bz\text{-}CB\text{-}TTDA)(H_2O)]^{2-}$ > MS-325 > $[Gd(CB\text{-}TTDA)(H_2O)]^{2-}$ > $[Gd(DTPA\text{-}BMA)(H_2O)]$ > $[Gd(DTPA)(H_2O)]^{2-}$. The ^{17}O $1/T_1$ relaxation rate curve for $[Gd(Bz\text{-}CB\text{-}TTDA)(H_2O)]^{2-}$ is higher than that of $[Gd(CB\text{-}TTDA)(H_2O)]^{2-}$, as shown in Figure 1B. This result implies that the benzyl group on the carbon backbone of $[Gd(Bz\text{-}CB\text{-}TTDA)(H_2O)]^{2-}$ is contributing to its τ_R^{298} value.[3] For the small-molecular weight Gd(III) complexes, the order of τ_R values is an index for proton relaxivity.

Ultrafiltration Studies of Gd(III) Chelates to HSA. The binding affinity of $[Gd(Bz\text{-}CB\text{-}TTDA)(H_2O)]^{2-}$ to HSA was evaluated by an ultrafiltration study across a membrane with a 30 kDa MW cutoff. It was assumed that the filtrate accurately represents the unbound $[Gd(Bz\text{-}CB\text{-}TTDA)(H_2O)]^{2-}$ in each sample. Concentrations of total $[Gd(Bz\text{-}CB\text{-}TTDA)(H_2O)]^{2-}$ in the initial solutions containing protein and in the filtrates were determined by

(66) Lincoln, S. F.; Merbach, A. E. *Adv. Inorg. Chem.* **1995**, *42*, 1–88.
(67) Tóth, E.; Helm, L.; Merbach, A. E.; Hedinger, R.; Hegetschweiler, K.; Janossy, A. *Inorg. Chem.* **1998**, *37*, 4104–4113.
(68) Muller, R. N.; Radüchel, B.; Laurent, S.; Platzek, J.; Piérart, C.; Mareski, P.; Vander Elst, L. *Eur. J. Inorg. Chem.* **1999**, 1949–1955.
(69) Brittain, H. G.; Desreux, J. F. *Inorg. Chem.* **1984**, *23*, 4459–4466.
(70) Abragam, A. *The Principles of Nuclear Magnetism*; Oxford University Press: London, 1961.
(71) Caravan, P.; Ellison, J. J.; McMurry, T. J.; Lauffer, R. B. *Chem. Rev.* **1999**, *99*, 2293–2352.
(72) Tóth, É.; Connac, F.; Helm, L.; Adzamli, K.; Merbach, A. E. *Eur. J. Inorg. Chem.* **1998**, 2017–2021.

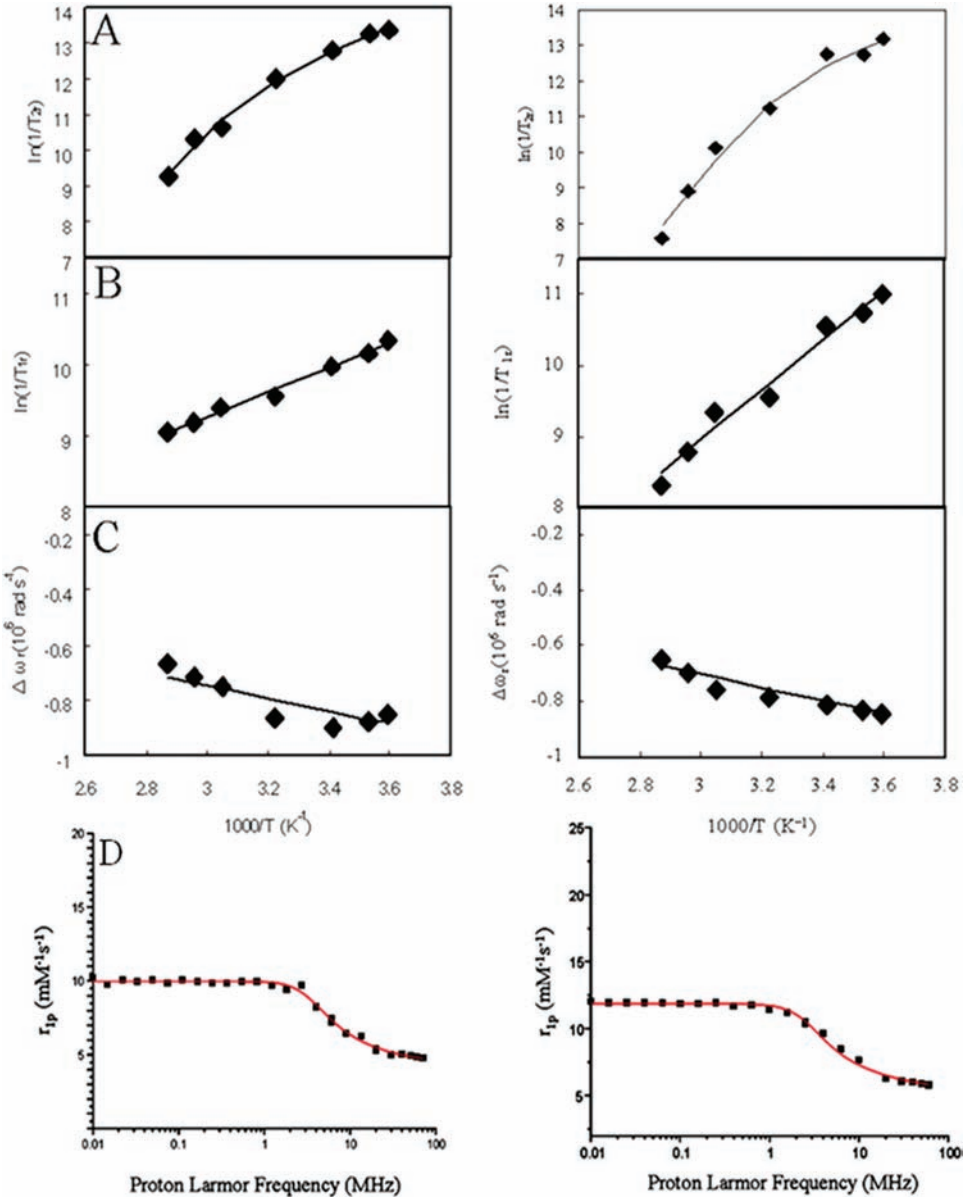

Figure 1. Temperature dependence of (A) transverse and (B) longitudinal ^{17}O relaxation rates; (C) ^{17}O chemical shifts at $B = 9.4$ T for [Gd(CB-TTDA)$(H_2O)]^{2-}$ (left) and [Gd(Bz-CB-TTDA)$(H_2O)]^{2-}$ (right). The lines represent simultaneous least-squares fits to all data points displayed. (D) NMRD profile (bottom) for [Gd(CB-TTDA)$(H_2O)]^{2-}$ (left) and [Gd(Bz-CB-TTDA)$(H_2O)]^{2-}$ (right).

measuring Gd(III) using ICP-MS. The extent of binding of [Gd(Bz-CB-TTDA)$(H_2O)]^{2-}$ to HSA is shown in Figure 2, and it represents the plot of the ratio of the bound [Gd(Bz-CB-TTDA)$(H_2O)]^{2-}$ per HSA molecule ($\bar{n}$) versus the concentration of unbound [Gd(Bz-CB-TTDA)$(H_2O)]^{2-}$. The value of $\bar{n}$ increases with the increase in molar concentration of unbound [Gd(Bz-CB-TTDA)$(H_2O)]^{2-}$. A complete binding curve is indicated by saturation plateau. The value at which $\bar{n}$ reaches the saturation plateau would represent the total number of occupied sites on HSA when it is saturated with GdL.[16] The saturation-like profile has not been observed at 1.3 equiv of bound [Gd(Bz-CB-TTDA)$(H_2O)]^{2-}$ per HSA. However, previous studies suggest that it is possible to fit the data to a stoichiometric model to estimate the stepwise binding constant.[73] The first three stepwise binding constants of Gd(Bz-CB-TTDA)$(H_2O)]^{2-}$ are shown in Table 6 together with [Gd(TTDA-BOM)$(H_2O)]^{2-}$ (TTDA-BOM = 6-carboxymethyl-benzyloxymethyl-3,10-di(carboxymethyl)-3,6,10-triazadodecanedioic acid) (Chart 1) and MS-325. From Table 6, we conclude that the affinity of [Gd(Bz-CB-TTDA)$(H_2O)]^{2-}$ to HSA is higher than that of [Gd(TTDA-BOM)$(H_2O)]^{2-}$ but is slightly lower than that of MS-325. Hence, the introduction of the benzyl and cyclobutyl groups into TTDA results in a strong binding of this GdL chelate to HSA.

Lipophilicity Study. Lipophilicity is well-known as a prime physicochemical descriptor of drug potency. As examples, drug absorption, plasma protein binding, and hydrophobic drug−receptor interactions are all correlated with lipophilicity. The lipophilic residue facilitates noncovalent interaction of MS-325 to the lipid binding

(73) Klotz, I. M. *Ligand Receptor Energetics-A Guide for the Perplexed*; John Wiley & Sons: New York, 1987.

Table 5. Kinetic and NMR Parameters of $[Gd(Bz\text{-}CB\text{-}TTDA)(H_2O)]^{2-}$, $[Gd(CB\text{-}TTDA)(H_2O)]^{2-}$, $[Gd(TTDA)(H_2O)]^{2-}$, $[Gd(EPTPA\text{-}bz\text{-}NO_2)(H_2O)]^{2-}$, [Gd(DTPA-BMA)$(H_2O)$], MS-325, and $[Gd(DTPA)(H_2O)]^{2-}$[a]

parameter	Bz-CB-TTDA	CB-TTDA	TTDA[b]	EPTPA-bz-NO_2[c]	DTPA-BMA[d]	MS-325[e,f]	DTPA[d]
k_{ex}^{298} (10^6 s^{-1})	271 ± 13	232 ± 14	146 ± 17	150 ± 40	0.45 ± 0.01	6.1	3.3 ± 0.2
$\Delta H^{\ddagger}$ (kJ mol^{-1})	23.1 ± 0.1	23.5 ± 0.4	23.1 ± 0.5	22.1 ± 1.8	47.6 ± 1.1	53.7	51.6 ± 1.4
$\Delta S^{\ddagger}$ (J mol^{-1} k^{-1})	−5.9 ± 0.3	−5.8 ± 1.0	−11.1 ± 3.1	−9.1 ± 5.0	22.9 ± 3.6	65	53.0 ± 4.7
$A/\hbar$ (10^6 rad s^{-1})	−3.5 ± 0.2	−3.7 ± 0.1	−3.2 ± 0.3	−3.2 ± 0.2[g]	−3.8 ± 0.2	−4.46	−3.8 ± 0.2
τ_R^{298} (ps)	*124* (151 ± 3)	*89* (112 ± 2)	104 ± 12	*122 ± 12*	*66 ± 11* (167 ± 5)	*110*[h] or *142*[h] (188)	*58 ± 11* (103 ± 10)
τ_v (10^{-11} s)	*5.73*	*4.91*		*2.2 ± 1*	*2.5 ± 1*	*2.2*	*2.5 ± 1*
r_{Gd-H} (Å)	**3.10**	**3.10**	**3.10**	**3.10**	**3.10**	**3.17**	**3.10**
Δ^2 (10^{18} s^{-2})	*8.31*	*1.14*		*40*	*41*	*7.1*	*46*
C_{os}	0	0	0		0.11 ± 0.04	0.23	0.18 ± 0.04
q	**1**	**1**	**1**	**1**	**1**	**1**	**1**
E_R (kJ mol^{-1})	27.2 ± 1.1	13.6 ± 0.8	24.8 ± 1.5	19.0 ± 1.7	21.9 ± 0.5	31.5	17.3 ± 0.8
method	^{17}O, NMRD	^{17}O, NMRD	^{17}O	^{17}O, EPR, NMRD	^{17}O,EPR, NMRD	^{17}O, NMRD	^{17}O, NMRD

[a] As obtained from the simultaneous fitting of ^{17}O NMR and NMRD data. [b] Data were obtained from ref 33. [c] Data were obtained from ref 44. [d] Data were obtained from ref 12. [e] Data were obtained from ref 16. [f] Data were obtained from ref 68. [g] The empirical constant for the outer-sphere contribution to the chemical shift was fixed at $C_{os} = 0.1$. [h] The first values correspond to the results of the fitting performed with r set to 0.295 nm, the second ones correspond to $r = 0.31$ nm. The τ_R^{298} values obtained by fitting only ^{17}O NMR data are given in parentheses. Bold values are fixed in the fit.

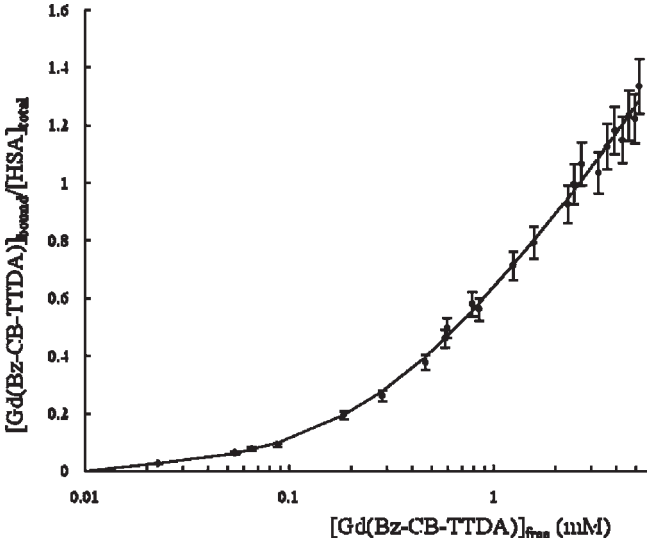

Figure 2. Plot of the ratio of bound $[Gd(Bz\text{-}CB\text{-}TTDA)(H_2O)]^{2-}$ per HSA versus the concentration of free $[Gd(Bz\text{-}CB\text{-}TTDA)(H_2O)]^{2-}$ (37.0 ± 0.1 °C, phosphate buffer, pH 7.4).

sites of HSA and significantly augments its plasma half-life. Hydrophilic−lipophilic balance (HLB) of the Gd(III) complex is a vital factor controlling the plasma half-life and elimination from the organism.[74] To augment the lipophilicity of the $[Gd(TTDA)(H_2O)]^{2-}$, we introduce lipophilic residues such as cyclobutyl and benzyl groups on the carbon backbone. The octanol−water distribution ratio, $K_{O/W}$, is the accepted physicochemical property measuring the hydrophobicity of Gd(III) complexes.[75,76] The log P (logarithm of partition coefficient in n-octanol/water) values can estimate the lipophilicity of a compound in a biological environment,[77] and thus, it is directly related to the binding affinity of Gd(III) complexes to HSA. The

Table 6. Association Constants for the Binding of $[Gd(Bz\text{-}CB\text{-}TTDA)(H_2O)]^{2-}$, $[Gd(TTDA\text{-}BOM)(H_2O)]^{2-}$, and MS-325 to HSA in Phosphate Buffer (pH 7.4) at 37.0 ± 0.1 °C

binding constant	[Gd(Bz-CB-TTDA)$(H_2O)]^{2-}$ (M^{-1})	[Gd(TTDA-BOM)$(H_2O)]^{2-}$ (M^{-1})[a]	MS-325 (M^{-1})[b]
K_{a1}	$(1.3 \pm 0.9) \times 10^3$	$(5.9 \pm 1.6) \times 10^2$	1.1×10^4
K_{a2}	$(1.0 \pm 0.7) \times 10^2$	$(0.9 \pm 0.3) \times 10^2$	8.4×10^2
K_{a3}	$(0.3 \pm 0.1) \times 10^2$		2.6×10^2
K_{a4}			4.3×10^2

[a] Data were obtained from ref 34. [b] Data were obtained from ref 16.

HPLC method is an indirect way to estimate log P values in the range of 0−6.[78] However, the HPLC chromatograms of $[Gd(CB\text{-}TTDA)(H_2O)]^{2-}$ and $[Gd(Bz\text{-}CB\text{-}TTDA)(H_2O)]^{2-}$ in the octanol phase could not be detected (data not shown). These results indicate that $[Gd(CB\text{-}TTDA)(H_2O)]^{2-}$ and $[Gd(Bz\text{-}CB\text{-}TTDA)(H_2O)]^{2-}$ have low lipophilicity.[75] Recently, several computer programs have been used to predict the lipophilicity of molecules. These programs are based on atom/fragment contributions, structural parameters, atom-type electrotopological-state indices, and topological structure descriptors.[79] We used the miLogP 1.2 online program[80] to calculate the log P values of TTDA, CB-TTDA, Bz-TTDA (4-benzyl-3,6,10-tri(carboxymethyl)-3,6,10-triazadodecanedioic acid),[37] Bz-CB-TTDA, and MS-325 ligand, and the values are shown in Table 7. The software calculates log P values as a sum of group contributions and correction factors. The sequence of increase in lipophilicity is TTDA < CB-TTDA < Bz-TTDA < Bz-CB-TTDA < MS-325 ligand. The trend in the increase of lipophilicity indicates that both cyclobutyl and benzyl residues contribute to the lipophilicity of ligands, and their cumulative effect on the lipophilicity can be observed in Bz-CB-TTDA. Furthermore, the partition coefficient of the $[Gd(Bz\text{-}CB\text{-}TTDA)(H_2O)]^{2-}$ complex was determined following a previously reported method.[41] The log P value of $[Gd(Bz\text{-}CB\text{-}TTDA)(H_2O)]^{2-}$ is −2.34 ± 0.15 which is

(74) Hifumi, H.; Tanimoto, A.; Honda, A.; Citterio, D.; Suzuki, K. *Anal. Sci.* **2007**, *23*, 1159–1165.
(75) Jastrzebska, B.; Lebel, R.; Therriault, H.; McIntyre, J. O.; Escher, E.; Guérin, B.; Paquette, B.; Neugebauer, W. A.; Lepage, M. *J. Med. Chem.* **2009**, *52*, 1576–1581.
(76) Sangster, J. *Octanol-Water Partition Coefficients, Fundamentals and Physical Chemistry*; John Wiley & Sons: Chichester, U.K., 1997.
(77) Van de Waterbeemd, H.; Gifford, E. *Nat. Rev. Drug Discovery* **2003**, *2*, 192–204.
(78) Chen, Z.; Weber, S. G. *Anal. Chem.* **2007**, *79*, 1043–1049.
(79) Medić-Sarić, M.; Mornar, A.; Jasprica, I. *Acta Pharm.* **2004**, *54*, 91–101.
(80) Molinspiration Cheminformatics Calculation of Molecular Properties and Drug-likeness. http://www.molinspiration.com (accessed 2009).

Table 7. log *p* Values for TTDA, CB-TTDA, Bz-TTDA, Bz-CB-TTDA, and MS-325 Ligand, Computed by miLogP 1.2 Computer Software

ligand	miLogP
TTDA	−5.539
CB-TTDA	−5.432
Bz-TTDA	−5.055
Bz-CB-TTDA	−4.875
MS-325 ligand	−4.575

slightly lower than that of MS-325 (−2.11 ± 0.06). This is consistent with ultrafiltration study which provides an accurate estimation of $[Gd(Bz\text{-}CB\text{-}TTDA)(H_2O)]^{2-}$ binding constants to HSA with a lower affinity than that of MS-325. This result implies that $[Gd(Bz\text{-}CB\text{-}TTDA)(H_2O)]^{2-}$ also has the optimum lipophilicity required for a blood pool agent. Excess lipophilic groups on the carbon backbone of $[Gd(TTDA)(H_2O)]^{2-}$ would have accelerated hepatobiliary excretion from the liver. The relevance of carbon backbone modification by appropriate lipophilic residues to impart optimum lipophilicity to Gd(III) complexes is clearly supported by the current findings.

Relaxivity Studies of Gd(III) Chelates to HSA. Macromolecular adducts formed as a result of noncovalent interaction of Gd(III) complexes to HSA have higher relaxivity than that of free Gd(III) complexes. Enhancement in the relaxivity upon binding to HSA is primarily because of remarkable reduction in the rotational diffusion rate of the molecules. In addition, binding of Gd(III) complexes to HSA slows down the renal excretion rate, and consequently, the prolonged blood plasma half-life facilitates the angiographic applications. The advantage of this concept is that a lesser amount of Gd(III) complex has to be injected into the patient. Moreover, the blood pool agent concentration remains relatively stable in plasma during examination and, consequently, allows imaging of multiple body regions without repeated doses. Hydrophobic residues as well as the negative electric charges are the basic requirement for binding of Gd(III) complexes to HSA.[81] The binding affinity of $[Gd(CB\text{-}TTDA)(H_2O)]^{2-}$ and $[Gd(Bz\text{-}CB\text{-}TTDA)(H_2O)]^{2-}$ to HSA was evaluated by proton relaxation enhancement method.[82] This technique allows us to obtain reliable and reproducible physical values such as the thermodynamic binding constant (K_A), the number of binding sites (n), and the bonded relaxivity (r_1^b) of the macromolecular adduct. The experimental procedure involves two distinct titrations, called E- and M-titration[83] (see the Supporting Information). The quantitative analysis of E-titration provides an accurate estimation of bound relaxivity (r_1^b) of Gd(III) complexes to HSA with higher affinity. However, E-titration is not sensitive to n particularly when K_A is small. The quantitative analysis of M-titration provides independent evaluation of K_A and n.[82] The results of E- and M-titrations for $[Gd(CB\text{-}TTDA)(H_2O)]^{2-}$ and $[Gd(Bz\text{-}CB\text{-}TTDA)(H_2O)]^{2-}$ in the presence of HSA are shown in Figures 3 and 4, respectively. $[Gd(Bz\text{-}CB\text{-}TTDA)(H_2O)]^{2-}$ displays steep enhancement in the longitudinal water proton relaxation rate upon addition of HSA owing to the formation of macromolecular adducts. On the other hand, the relaxation rate enhancement shown by $[Gd(CB\text{-}TTDA)(H_2O)]^{2-}$ is much less in the presence of HSA and increases linearly with concentration, which reflects weak protein interaction.[83] This result implies that the HSA has higher affinity for $[Gd(Bz\text{-}CB\text{-}TTDA)(H_2O)]^{2-}$ than $[Gd(CB\text{-}TTDA)(H_2O)]^{2-}$. The high affinity of HSA toward $[Gd(Bz\text{-}CB\text{-}TTDA)(H_2O)]^{2-}$ can be explained in terms of hydrophobicity. The co-presence of benzyl and cyclobutyl moieties in $[Gd(Bz\text{-}CB\text{-}TTDA)(H_2O)]^{2-}$ induces much higher hydrophobicity than cyclobutyl alone in $[Gd(CB\text{-}TTDA)(H_2O)]^{2-}$. The effect of hydrophobicity of the Gd(III) complex on the affinity toward HSA can be evaluated by comparing the K_A value of the Gd(III) complex.[84] The K_A value of $[Gd(Bz\text{-}CB\text{-}TTDA)(H_2O)]^{2-}$ is almost 1 order of magnitude higher than that of $[Gd(CB\text{-}TTDA)(H_2O)]^{2-}$. The binding parameters of $[Gd(CB\text{-}TTDA)(H_2O)]^{2-}$ and $[Gd(Bz\text{-}CB\text{-}TTDA)(H_2O)]^{2-}$ calculated for the single binding site (n = 1) on HSA are presented in Table 8, along with those of other linear

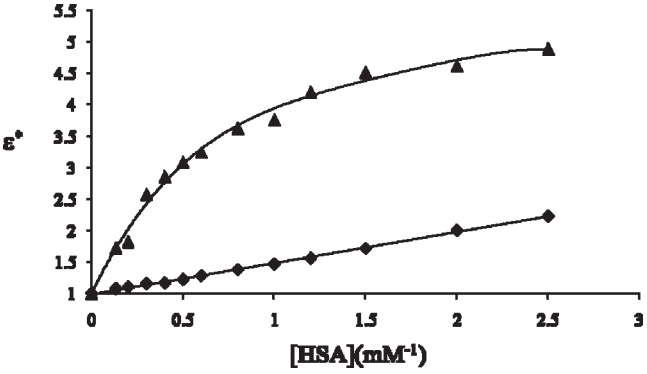

Figure 3. E-titration of a 0.1 mM solution of $[Gd(Bz\text{-}CB\text{-}TTDA)(H_2O)]^{2-}$ (▲) and $[Gd(CB\text{-}TTDA)(H_2O)]^{2-}$ (◆) with HSA (20 MHz, 25.0 ± 0.1 C, 50 mM phosphate buffer, pH 7.4). The solid curves represent the best fit.

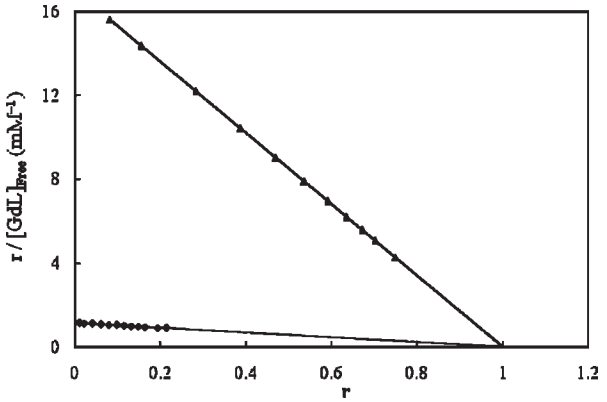

Figure 4. Scatchard plot of the data obtained from the PRE titration of a 0.6 mM HSA solution (pH 7.4, HEPES buffer, 25.0 ± 0.1 °C, 20 MHz) with $[Gd(Bz\text{-}CB\text{-}TTDA)(H_2O)]^{2-}$ (▲) and $[Gd(CB\text{-}TTDA)(H_2O)]^{2-}$ (◆); r = [GdL-HSA]/$[HSA]_T$.

(81) Peters, T. J. *All About Albumin: Biochemistry, Genetics, and Medical Applications*; Academic Press: San Diego, CA, 1996.
(82) Dwek, R. A. *Nuclear Magnetic Resonance in Biochemistry, Application to Enzyme System*; Clarendon Press: Oxford, 1973.
(83) Aime, S., Fasano, M., Terreno, E., Botta, M., Eds. *The Chemistry of Contrast Agents in Medical Magnetic Resonance Imaging*; John Wiley and Sons: New York, 2001; pp 193−241.
(84) Aime, S.; Botta, M.; Fasano, M.; Geninatti Crich, S.; Terreno, E. *J. Biol. Inorg. Chem.* **1996**, *1*, 312–319.
(85) Aime, S.; Chiaussa, M.; Digilio, G.; Gianolio, E.; Terreno, E. *J. Biol. Inorg. Chem.* **1999**, *4*, 766–774.

Table 8. Binding Parameters to HSA from PRE Measurements (25.0 ± 0.1 °C, 20 MHz, pH 7.4, 50 mM Phosphate Buffer)[a]

complexes	K_A (M^{-1})	n	ε_b	r_1^{free} ($mM^{-1}\ s^{-1}$)	r_1^b ($mM^{-1}\ s^{-1}$)
$[Gd(Bz\text{-}CB\text{-}TTDA)(H_2O)]^{2-}$	$(1.5 \pm 0.1) \times 10^3$	1	13.1 ± 0.4	5.1 ± 0.3	66.7 ± 2.2
$[Gd(CB\text{-}TTDA)(H_2O)]^{2-}$	$(1.1 \pm 0.1) \times 10^2$	1	6.1 ± 0.2	4.8 ± 0.1	29.3 ± 0.8
$[Gd(TTDA\text{-}BOM)(H_2O)]^{2-}$[b]	$(4.6 \pm 0.1) \times 10^2$	1	13.7 ± 0.1	4.8 ± 0.02[c]	65.8 ± 2.7
$[Gd(BOPTA)(H_2O)]^{2-}$[c]	$(4.0 \pm 0.1) \times 10^2$				33
MS-325[d]	$(3.0 \pm 0.2) \times 10^4$	1		6.6 ± 0.4[c]	47.0 ± 4

[a] $K_A = [GdL - HSA]/[GdL]_F[nHSA]_F$, where [*n*HSA] represents the binding sites concentration, the subscripts T and F refer to "total" and "free" species, respectively. $r_1^b = \varepsilon_b \times r_1^{free}$, where, ε_b refers to maximum value of the enhancement factor ε^*, and r_1^{free} and r_1^b refer to the relaxivity of free and bound complex, respectively. [b] Data were obtained from ref 34. [c] Data were obtained from ref 84. [d] Data were obtained from ref 85.

poly(aminocarboxylate) complexes. The K_A value for $[Gd(Bz\text{-}CB\text{-}TTDA)(H_2O)]^{2-}$ is lower than that of MS-325 but is higher than those of $[Gd(CB\text{-}TTDA)(H_2O)]^{2-}$, $[Gd(TTDA\text{-}BOM)(H_2O)]^{2-}$, and $[Gd(BOPTA)H_2O]^{2-}$ (BOPTA = 4-carboxy-5,8,11-tris(carboxymethyl)-1-phenyl-2-oxa-5,8,11-triazatridecan-13-oic acid). The bound relaxivity (r_1^b) of $[Gd(Bz\text{-}CB\text{-}TTDA)H_2O]^{2-}$ obtained by multiplying b and r_1^F is significantly higher than that of MS-325, which can be explained in terms of the water exchange rate on these two Gd(III) complexes. The water exchange rate on the Gd(III) complex generally slows down by a factor of 2−3-fold upon binding to HSA.[16] The decrease in water exchange rate upon binding to HSA may be more effectively borne by $[Gd(Bz\text{-}CB\text{-}TTDA)(H_2O)]^{2-}$ than by MS-325, owing to higher water exchange rate on $[Gd(Bz\text{-}CB\text{-}TTDA)(H_2O)]^{2-}$ ($271 \times 10^6\ s^{-1}$) than that of MS-325 ($5.8 \times 10^6\ s^{-1}$).

Transmetalation. The stability of $[Gd(Bz\text{-}CB\text{-}TTDA)(H_2O)]^{2-}$ and $[Gd(CB\text{-}TTDA)(H_2O)]^{2-}$ complexes against the presence of Zn(II) ions was determined by transmetalation experiments carried out in phosphate buffer (pH 7.4) in the presence of $ZnCl_2$ as the competing ionic species. Replacement of Gd(III) in the complex with Zn(II) leads to free gadolinium ions, which precipitate out in the presence of phosphate as $GdPO_4$, and consequently, the total amount of paramagnetic species in solution decreases.[86] The estimation of the decrease in relaxivity allows us to track the transmetalation reaction. The two characteristic values can be used to describe the behavior of a Gd(III) chelate in a transmetalation experiment: the time to reach $R_1^m/R_{1,0} = 0.8$ (the ratio index) which gives information about the kinetics of the reaction and $R_1^m(t)/R_1^m(0)$ value at very long time, $t = \infty$ (the long time index, considered after 3 days), that reflects the thermodynamic aspect of the system (R_1^m and $R_{1,0}$ are the relaxation rate at time t and at time 0, respectively).[42,43] The percentages of Gd(III) complexes left in the solution after 3 days for $[Gd(Bz\text{-}CB\text{-}TTDA)(H_2O)]^{2-}$ and $[Gd(CB\text{-}TTDA)(H_2O)]^{2-}$ are summarized in Table 9 together with $[Gd(TTDA\text{-}BOM)(H_2O)]^{2-}$, $[Gd(DTPA)(H_2O)]^{2-}$, and $[Gd(DTPA\text{-}BMA)(H_2O)]^{2-}$. Figure 7S in the Supporting Information shows $R_1^m(t)/R_1^m(0)$ versus time for $[Gd(DTPA)(H_2O)]^{2-}$, $[Gd(CB\text{-}TTDA)(H_2O)]^{2-}$, and $[Gd(Bz\text{-}CB\text{-}TTDA)(H_2O)]^{2-}$. The transmetalation reaction rate for $[Gd(Bz\text{-}CB\text{-}TTDA)(H_2O)]^{2-}$, $[Gd(CB\text{-}TTDA)(H_2O)]^{2-}$, $[Gd(TTDA\text{-}BOM)(H_2O)]^{2-}$, and $[Gd(DTPA)(H_2O)]^{2-}$ is similar and is five times slower than that of $[Gd(DTPA\text{-}BMA)(H_2O)]^{2-}$. This result implies that $[Gd(Bz\text{-}CB\text{-}TTDA)(H_2O)]^{2-}$ and $[Gd(CB\text{-}TTDA)(H_2O)]^{2-}$ are fairly stable with respect to transmetalation. Therefore, the kinetic and thermodynamic stabilities of $[Gd(Bz\text{-}CB\text{-}TTDA)(H_2O)]^{2-}$ and $[Gd(CB\text{-}TTDA)(H_2O)]^{2-}$ are stable enough to be used as contrast agents for MRI.

Table 9. Values of R_1^m (t = 3 d)/R_1^m (t = 0) for the Gd(III) Complexes after 3 Days of Transmetalation with Zn(II) at 20 MHz and 37.0 ± 0.1 °C

complex	R_1^m (t = 3 d)/R_1^m(t = 0) (%)
$[Gd(Bz\text{-}CB\text{-}TTDA)(H_2O)]^{2-}$	46.14
$[Gd(CB\text{-}TTDA)(H_2O)]^{2-}$	47.40
$[Gd(TTDA\text{-}BOM)(H_2O)]^{2-}$[a]	43.90
$[Gd(DTPA)(H_2O)]^{2-}$[a]	49.79
$[Gd(DTPA\text{-}BMA)(H_2O)]$[b]	9.00

[a] Data were obtained from ref 34. [b] Data were obtained from ref 43.

Conclusion

We have synthesized and characterized two TTDA derivatives which possess cyclobutyl and/or benzyl moieties. Both complexes, $[Gd(CB\text{-}TTDA)(H_2O)]^{2-}$ and $[Gd(Bz\text{-}CB\text{-}TTDA)(H_2O)]^{2-}$, display high stability constants, and CB-TTDA and Bz-CB-TTDA show superior selectivity of Gd(III) against Zn(II) than TTDA and DTPA but inferior to MS-325. The simultaneous treatment of ^{17}O NMR and NMRD data is used to obtain several parameters affecting the proton relaxivity of Gd(III) complexes. It is found that the introduction of the cyclobutyl group increases the steric constraint at the water binding site and thereby increases the water exchange rate of $[Gd(Bz\text{-}CB\text{-}TTDA)(H_2O)]^{2-}$ and $[Gd(CB\text{-}TTDA)(H_2O)]^{2-}$. From the ultrafiltration studies, $[Gd(Bz\text{-}CB\text{-}TTDA)(H_2O)]^{2-}$ has a higher affinity to HSA than $[Gd(TTDA\text{-}BOM)(H_2O)]^{2-}$ but is slightly lower than MS-325. However, the r_1^b value of the $[Gd(Bz\text{-}CB\text{-}TTDA)(H_2O)]^{2-}$ complex has a remarkably high value with HSA. The kinetic stability of $[Gd(CB\text{-}TTDA)(H_2O)]^{2-}$ and $[Gd(Bz\text{-}CB\text{-}TTDA)(H_2O)]^{2-}$ complexes toward transmetalation with Zn(II) is similar to that of $[Gd(DTPA)(H_2O)]^{2-}$. Therefore, $[Gd(Bz\text{-}CB\text{-}TTDA)(H_2O)]^{2-}$ may potentially be used as a blood pool contrast agent for MRI.

Acknowledgment. Funding from National Science Council of Taiwan (Grant Nos. NSC 98-2627-M-009-009 and NSC 97-2113-M-009-016-MY3) is gratefully acknowledged.

Supporting Information Available: Additional experimental details, figures, and tables. This material is available free of charge via the Internet at http://pubs.acs.org.

Note Added after ASAP Publication. This paper was published ASAP on January 19, 2011, with errors in production that included the absence of Schemes 1 and 2 and part of Figure 1. The corrected version was published on January 25, 2011.

(86) Moriggi, L.; Cannizzo, C.; Prestinari, C.; Berrière, F.; Helm, L. *Inorg. Chem.* **2008**, *47*, 8357–8366.